

Design and Fabrication of a 50mm Gun Launched Hybrid Projectile

Mr. Saul Henderson, University of the District of Columbia

Saul Henderson is a first-year Master's student within the Electrical Engineering department at the University of the District of Columbia (UDC). Prior to joining the Master's program in August 2019, Saul has gained over 6 years of valuable experience and soft skills in STEM research, design and informal education. Starting out at UDC as an undergraduate Electrical Engineering student in the Fall of 2012, he has gained 5 years of education experience as a student educator at the Smithsonian National Air and Space Museum (NASM). As an educator at a world-class museum, he was responsible for interacting with several hundred to thousands of visitors daily by educating them on the basic principles of aerodynamics, flight systems and space travel. Saul has also spent 2 years of his undergraduate career as a research assistant in several areas including Machine Learning, Power Systems and Mechatronics. In this capacity, he spent most of his time working under his school dean, Dr. Devdas Shetty, to enhance labs and higher-level coursework through the use of hands-on mechatronics projects and robotics. He has also worked briefly in other UDC labs including the Center for Biomedical & Rehabilitation Engineering (CBRE) and the upcoming Smart Grid lab. Saul has recently obtained his B.S in Electrical Engineering with a concentration in Computer Engineering from UDC in May 2019, where he graduated with honors. Immediately upon starting the Master's program, Saul has completed an internship in solar design where he assisted in the preliminary design and energy modeling of several dozen sites for major companies across the eastern United States. Saul is currently a graduate research assistant focusing on Wireless Communications and Cyber-Physical Systems.

Dr. Sasan Haghani, University of the District of Columbia

Sasan Haghani, Ph.D., is an Associate Professor of Electrical and Computer Engineering at the University of the District of Columbia. His research interests include the application of wireless sensor networks in biomedical and environmental domains and performance analysis of communication systems over fading channels.

Dr. Esther T. Ososanya, University of the District of Columbia

Dr. Esther T. Ososanya is a professor of Electrical and Computer Engineering at the University of the District of Columbia, and the current department chairperson. During her career, Dr. Ososanya has worked for private industry as a circuit development engineer and as a software engineer, in addition to her academic activities. She received her education in the United Kingdom, where she achieved her Ph.D. in Electrical Engineering from the University of Bradford in 1985, and a Post Doctoral Research Fellow from the University of Birmingham, UK. She was a Visiting Professor at Michigan Technological University for five years, and an Associate professor at Tennessee Technological University for 7 years prior to arriving at the University of the District of Columbia in the Fall of 2001. Dr. Ososanya research interests include new applications for VLSI ASIC design, Microcomputer Architecture, Embedded Systems design, Nanotechnology, and Renewable Energy Systems. In recent years, she has worked with colleagues to apply these technologies to Biomass research, Solar Cells efficiency capture research, and Renewable Energy Curriculum developments.

Dr. Devdas Shetty, University of the District of Columbia

Dr. Devdas Shetty Dean, School of Engineering and Applied Science Professor of Mechanical Engineering University of the District of Columbia 4200 Connecticut Ave. NW Washington, DC 20008; Tel: 202 274 5033(off) Email: devdas.shetty@udc.edu

Dr. Devdas Shetty serves as dean of the School of Engineering and Applied Sciences at the University of the District of Columbia, where he is also a Professor of Mechanical Engineering. Dr. Shetty previously served as Dean of Engineering at Lawrence Technological Institute, MI and Dean of Research at the University of Hartford, CT. At the University of Hartford he was the founding chair-holder of the distinguished Vernon D. Roosa Endowed Professorship. As the Director of the Engineering Applications

Center, he had set up partnership with more than 50 industries. He also held positions at the Albert Nerkin School of Engineering at the Cooper Union for the Advancement of Science and Art in New York City.

Dr. Shetty is the author of 3 books, and more than 225 scientific articles, and papers. His textbooks on Mechatronics and Product Design are widely used around the world. His work has been cited for contribution to the understanding of surface measurement, intellectual achievements in mechatronics and contributions to product design. He has five Patents for inventions that involve interdisciplinary areas of mechanical engineering, design and computer science. Dr. Shetty has led several successful multi institutional engineering projects. In partnership with Albert Einstein College, he invented the mechatronics process for supporting patients with ambulatory systems for rehabilitation. Major honors received by Professor Shetty include the James Frances Bent Award for Creativity, the Edward S. Roth National Award for Manufacturing from the Society of Manufacturing Engineers, the American Society of Mechanical Engineer Faculty Award, and the Society of Manufacturing Engineers Honor Award. He is an elected member of the Connecticut Academy of Science and Engineering, and the Connecticut Academy of Arts and Sciences. He also is the author of Mechatronics System Design, published by Cengage Learning, now in its second edition.

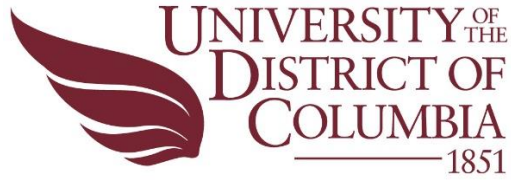
CO-AUTHORS

Dr. Suhash Ghosh Assistant Professor, Mechanical Engineering University of Hartford, Connecticut, CT 06107 &

Prof. Claudio Campana Research Engineer Engineering Applications Center University of Hartford, West Hartford, CT 06117

Christopher Riso, University of the District of Columbia

Mr. Rudy Antonio Villegas



Design, Fabrication, and Testing of a 50mm Gun Launched Hybrid Projectile

Christopher Riso, Christopher Carter, Rudy Villegas and Heungmin Park

Department of Mechanical Engineering
School of Engineering and Applied Sciences
University of the District of Columbia

Saul Henderson

Department of Electrical and Computer Engineering
School of Engineering and Applied Sciences
University of the District of Columbia

Advisors:

Dr. Devdas Shetty, Dr. Jiajun Xu, Dr. Esther Ososanya, Dr. Sasan Haghani

School of Engineering and Applied Sciences
University of the District of Columbia

THIS PAGE INTENTIONALLY LEFT BLANK

Table of Contents

Abstract.....	3
Introduction.....	4
Methodology	5
Projectile Assumptions, Objectives, and Requirements	9
Aerodynamic Considerations.....	11
Forces.....	11
Nose Cone Design	12
Wing Design and Wing Actuation.....	14
Tail Design and Fin Actuation.....	15
Aerodynamic Equations.....	18
Results.....	19
Trajectory	
Simulation Procedure.....	21
Manufacturing of Components	
Nose Cone	
Tail and Tail Fins	
Wing System	
Electrical	25
System Requirements	25
Closed-loop Feedback System.....	27
Power System	27
Surveillance System	28
Information System	28
Communication System.....	28
Actuation System.....	28
Ground System	29
Arduino Micro	29
Assembly and Testing	
Bill of Materials	32
Gantt Chart.....	34

Fall Semester	34
Winter Semester.....	35
Future Work	36
Appendix	
References.....	38

List of Figures

1. Figure 1. Morphology Chart	6
2. Figure 2. QFD Chart	7
3. Figure 3. S.W.O.T Analysis	8
4. Figure 4. Design Structural Matrix.....	8
5. Figure 5. Design Decision Matrix.....	9
6. Figure 6. Nose Cone Dimension Design 1.....	13
7. Figure 7. Nose Cone Dimension Design 2.....	13
8. Figure 8. Nose Cone 3D Design	14
9. Figure 9. Tail 3D Design	16
10. Figure 10. Tail Dimension Design	16
11. Figure 11. Fin Dimension Design 1	17
12. Figure 12. Fin Dimension Design 2	17
13. Figure 13. Center of gravity and pressure	20
14. Figure 14. Coefficient of Drag Vs. Ma.....	21
15. Figure 15. Velocity Distribution.....	23
16. Figure 16. Velocity Distribution AoA=-2	24
17. Figure 17. Pressure Distribution.....	24
18. Figure 18. A general idea of the control system for the UAV	26
19. Figure 19. L16-R servo (68 mm L x 18 mm W x 20 mm)	29
20. Figure 20. Arduino Micro Rear	29
21. Figure 21. Arduino Micro Front.....	29
22. Figure 22, Arduino Micro Pinout.....	30
23. Figure 23. Electrical system flow chart.....	31

List of Tables

1. Table 1. Aerodynamic Analysis Calculation Result Table	19
---	----

1. Abstract

Unmanned Aerial Vehicles (UAV) have provided the military with the ability to strike targets and gather intel without risking the lives of human operators. This project will detail the design, analysis, and fabrication of a UAV. The objective is to design a UAV with the ability to extend its range and gain increased maneuverability in order to accurately strike a target from a greater distance away. This is a multidisciplinary complex task with many different considerations. The projectile must be outfitted with wings that are initially housed within its body to ensure that it is able to be fired from an existing gun. The body of the projectile must be designed for aerodynamic feasibility. The electrical system of the missile guidance project is very critical as it is responsible for guiding the missile to its target, providing surveillance and controlling the actuators. The electrical system of the missile will contain four major systems: actuation, surveillance, communications and positioning. Because of the size and weight constraints of the missile, the Arduino Mini microcontroller will be used to gather data from smaller sensors and provide actuation due to its small size and ease of use.

2. Introduction

The guided hybrid projectile is an unmanned aerial vehicle (UAV) that can be launched from a pre-existing gun. This projectile will be 50mm in diameter and designed to be lightweight (<1.5 kg) thus ensuring that it is portable, so it can be utilized by soldiers on the ground. This projectile will be outfitted with: guidance system, real-time video feedback, and an electromechanical wing actuating system. Live feedback will be sent between projectile and ground base to keep track of flight path. The use of the electromechanical wing actuating system will effectively extend the range of a standard ballistic projectile. The wings will also give the projectile the capabilities of in-flight self-correcting measures to ensure precise target acquisition. The in-flight actuation will occur at the apogee of the flight path in attempt to maximize the range of the projectile [1]. Without a human operator, the projectile will rely on aerodynamic forces to provide lift. As the wing area is increased, the range can be maximized. However, there will be less room to house the essential guidance and feedback mechanisms, as well as the electromechanical actuation system. The analysis of the aerodynamic forces will be done through calculation, simulation, and then wind tunnel testing.

The electro-mechanical system developed to maneuver the UAV uses a series of sensors & servo-motors executed by an Arduino Software (IDE) implemented on a printed circuit board (PCB). Live video feedback transmitted between projectile and ground base via an RF communication's link with an altitude sensor working alongside a 6-axis gyroscope assists in the projectiles' automatic flight guidance system. All internal components must be designed for the overall survivability of gravitational forces inherent to high speed travel.

3. Methodology

The project idea was inherited from previous years' Senior Capstone project (Fall 2017 – Spring 2018) using insightful knowledge on how the previous team developed their wing actuation mechanism as well as their electronic topology within the projectile. A complete overhaul is required with the only similarity between the projects is that the projectile is gun launched. A redesign of the nosecone, air-frame, wing-actuation mechanism, and tail-fin; along with the electrical components such as: telemetry sensors, micro-controllers, linear actuators, camera, and communications have to be re-defined to conform with the new 50mm projectile architecture along with new size and space constraints.

We have determined to implement the use of GANTT charts, morphological chart, quality functional development (QFD) diagrams, S.W.O.T. Chart, Design Decision Matrix, and a Design Structural Matrix in order to evaluate all the possible outcomes for the feasibility of acquiring the final product [2]. It should also be noted that patching guidelines were followed along the path of progression within the project. These patching guidelines allowed team members solve problems encountered in the developmental phase of the project, those mostly used were the combining, decomposing, rearrangement, and substitution guidelines [2].

The first step in evaluating the electrical systems and mechanical components was to implement a morphological chart for all the possible components and combinations of them all.

Attributes	Solutions				
Telemetry Sensors	Proximity Sensors	GPS Sensors	Inertial Reference System	Altimeter	Accelerometer
Wing Actuation	Fixed Wing	Spring loaded wing	Servo-Assisted extending outward	Worm-Gear Mechanism	3 or 4 bar linkage mechanism
Air-Frame	Cylindrical Body, no perforations.	Cylindrical body, metal – slotted exit for wings	Cylindrical Body, frontal surface area of wing shaped to accommodate curvature of outer body diameter	Cylindrical Body, rubber flap allowing extension of wings	
Tail	Fixed Tail Wings	Fixed tail wings with an extension that rotates about a pin located on-top of tail fin	Spring-assisted tail fins		

Figure 1. Morphology Chart

The highlighted cells in Figure 1. are what the team agreed upon in terms of mechanical structure and electrical elements thus far.

Moving on to the quality function diagram, it allowed us to correlate functional requirements of the guided projectile with the “customer” requirements, if you will. Referring to Fig. 2, the top triangle indicates the correlation between all of the functional requirements, whereas the body of the chart is the interrelationship between the functional and customer requirements on a scale of strong, moderate, to weak.

Correlations	
Positive	+
Negative	-
No Correlation	

Relationships	
Strong	●
Moderate	○
Weak	▽

Direction of Improvement	
Maximize	▲
Target	◇
Minimize	▼

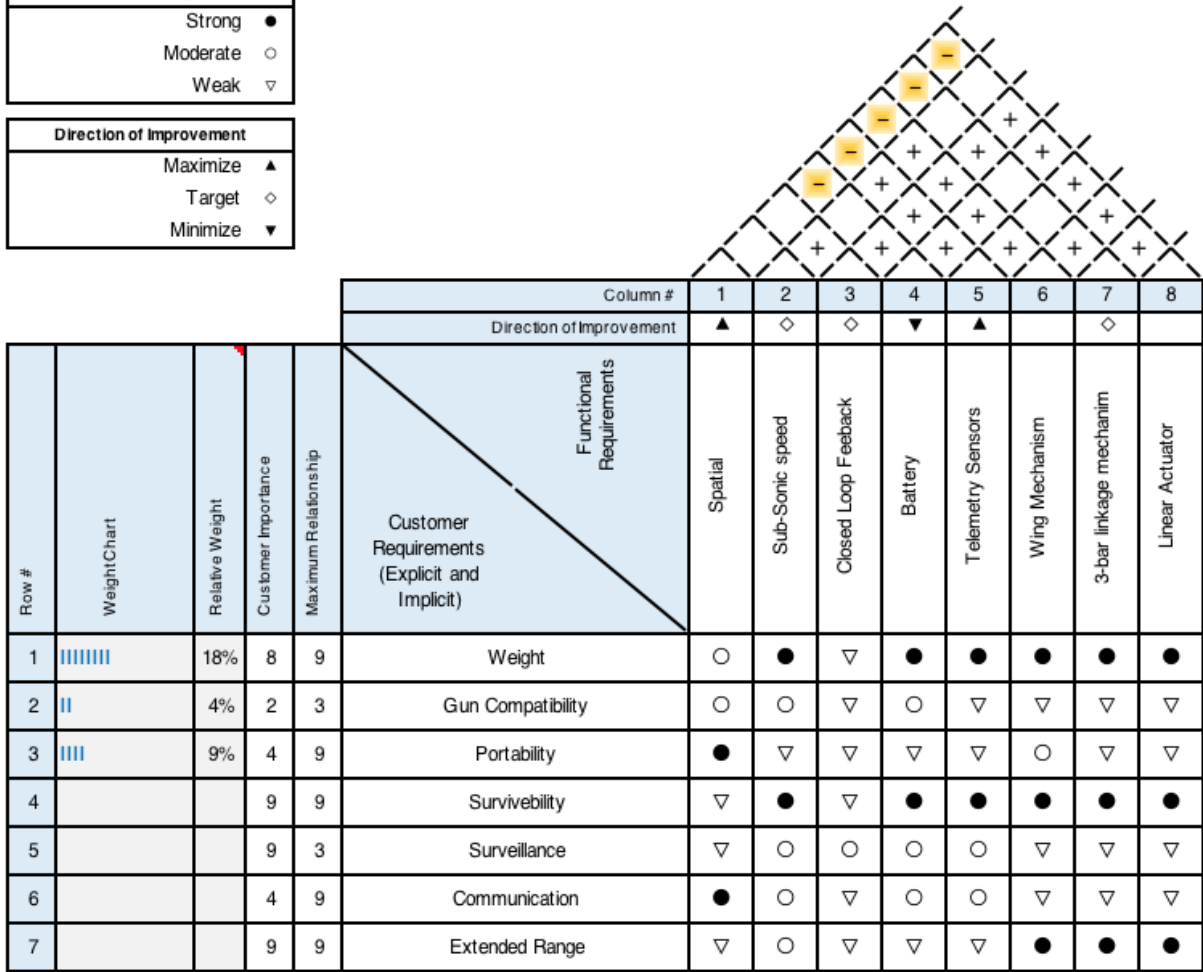


Figure 2. QFD Chart

This assessment helps to prioritize where maximum attention to detail should be focused on.

S.W.O.T. Analysis:

Hybrid Electro-Mechanical Projectile

Strengths

- Physical Resources
- Activities & Processes
- Human Resources

Weaknesses

- Financial
- Past Experience

Opportunities

- Future Trends

Opportunity & Strengths

- 3-D Print metal & composite components
- Rapid prototyping includes a modular design
- Electrical Engineering Expertise
- Mechanical Engineering Expertise

Opportunity & Weaknesses

- Electro-Mechanical systems allow for maneuverable components & telemetry.
- Emerging technologies will source funding for further research & development

Threats

- Funding

Threat & Strengths

- Recycle used electrical components from past projects for development & allow for re-usability during testing for reliability testing.
- Composite 3-D printer will be used for physical model analysis & wind tunnel testing.

Threat & Weaknesses

- Being well aware of previous failures to save time and resources.

Figure 3. S.W.O.T. Analysis

Functions		1	2	3	4	5	6	7
1	Select Target Coord.	1			1	1		1
2	Launch		1	1	1	1	1	1
3	Fin Actuation			1				1
4	Feedback Tele.				1			
5	Telemetry					1	1	1
6	Wing Actuation						1	1
7	Guided Flight							1

Figure 4. Design Structural Matrix

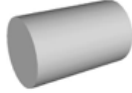


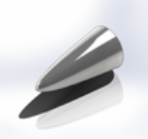

Criteria	Weight	Blunted Cylinder (Datum) 	Ogive 	Bi-Conical 	Power Series ½ 	Cone 
Coefficient of Drag	x3	1	3	2	5	3
L/D Ratio	x3	1	4	2	4	3
Manufacturability	x3	5	3	2	3	4
Piercing Ability	x1	1	5	4	3	4
Aesthetic	x1	1	4	2	4	1
Camera Mount-ability	x2	5	3	2	4	1
Weighted Total		33	45	28	51	37

Figure 5. Design Decision Matrix

4. Projectile Assumptions, Objectives, and Requirements

The initial task was to document a clearly defined set of program objectives and requirements. The projectile must be able to achieve an extended range while being able to maneuver with a real time feedback system. This projectile must be designed with a 50 mm diameter. In addition to the system requirements the projectile must be low cost with manufacturability. Based on these objectives the following set of requirements and assumptions were established to ensure design functionality:

- (1) Acceleration due to gravity is constant ‘g’ is constant both in magnitude and direction.
- (2) The free-fall acceleration is constant over the range of motion.

* It is directed downwards.

* Its reasonable if the range is small compared to the radius of the earth.

(3) With these assumptions, an object that is in projectile motion will follow a parabolic path called trajectory.

(4) Outer Diameter (D) = 50 mm

(5) Length of UAV $\sim 10(D) = 10(50) = 500$ mm

(6) Nosecone = $2(D) = 2(50) = 100$ mm

(7) Can be loaded into a gun with a Muzzle Velocity = 60-170 m/s

(8) Gun will be smooth bore

(9) Range = 400 m

(10) Ability to operate in wind conditions of 8 m/s (max magnitude in any one direction i.e. crosswind, headwind)

(11) Expected setback force of 5,000 G

(12) Cost of $< \$500$ at 10,000 volume of production

(13) Total Mass of < 1.5 kg

(14) Projectile with a minimum of 30 seconds of flight time after reaching apogee

5. Aerodynamic Considerations

5.1 Aerodynamic Forces

Without any propellant the projectile will only gain velocity from the initial launch from the gun. After this, it must rely on aerodynamic forces in order to extend its range. The two main forces that will be focused on for this project are lift and drag. Only with a solid understanding of these two forces can we proceed any further and begin to design the profile of the projectile.

Drag is the aerodynamic force that opposes the objects motion through a fluid. It is generated by the interaction of a solid in a fluid and is also generated at every part of the object. It is a vector force with both a magnitude and direction and requires both fluid and motion to exist. Often, when designing a projectile one of the main goals is to minimize the drag force. There are many ways to reduce the drag force such as choosing an optimum shape for a given speed [8].

Lift is the aerodynamic force that opposes the weight of an object. Like drag, lift is generated by every part of the projectile, however, the primary source of the lift generation is from the wings. Lift is also a vector and requires both fluid and motion in order to exist. The lift is generated by a pressure variance that is created when a fluid passes over the top and the bottom of the wing. It essentially works based on Bernoulli's equation. The ways to increase lift mostly stem from the increased area of the wings with an airfoil design that contributes very little to the drag force and provides a great increase in the lift force [9].

For the scope of this report we will be attempting to design the external configuration of the projectile to have minimal drag and maximum lift. The focus of the minimization of the drag will be on the shape of the nose cone and the overall projectile profile. Based off the size and

internal housing requirement we have a significant constraint on the ability to design an optimum lift producing wing. We will not have the luxury of creating an optimal airfoil shape, as the wing must be housed inside of the projectile and the wings profile will follow the same curvature as the body of the projectile. With this limitation the goal will be to maximize the aspect ratio. Since the wing is housed in the body for the first stage of flight, we will attempt to manufacture tail fins that can generate lift immediately after launch. Upon the actuation of the wing we wish to convert our ballistic flight to gliding flight. Our goal for design is to produce a high lift to drag ratio in order to initiate the gliding flight path upon actuation.

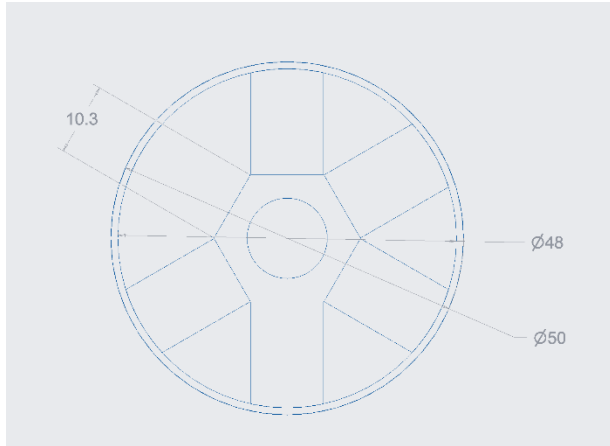
5.2 Nose Cone Design

The goal in the nose cone design is to minimize the total drag force induced on the projectile. The coefficient of drag is a direct result of the shape of the nose cone. Different speeds and Mach numbers require different shapes for the nose cone. When selecting the shape, the two considerations will be manufacturability and coefficient of drag for that particular shape. The projectile launched with an initial speed of 170 m/s will be exposed to a Mach number of 0.5. This is described as subsonic travel. Rounded nose cones (i.e. with an elliptical or paraboloidal profile) offer the lowest drag at subsonic speeds [8]. The $\frac{1}{2}$ power series nose cone was chosen as it has the lowest coefficient of drag for this regime and is relatively simple for ease of fabrication. The blunted tip is optimal for drag reduction at $Ma = 0.5$. The power series nose profile is generated by the following equation:

$$5.1 \quad y = R \left(\frac{x}{L} \right)^n$$

Where $R = \text{radius}$, $L = \text{Length}$, and $n = 0.5$ for $0 < x < 100$

This piece will be machined out of 6061 general purpose aluminum in the University of the District of Columbia machine shop. It will extend past the base of the nose by 25mm in order to make a secure connection to the body. Threaded inserts will be attached to this extension. It is



paramount that the nose cone has near perfect geometric symmetry. Any deviations from the curve can result in the projectile not travelling straight thus reducing the maximum range [8]. This will be a manufacturing challenge for next semester where we must explore the machining options for a high tolerance piece.

Figure 6. Nose Cone Dimension Design 1



Figure 7. Nose Cone Dimension Design 2

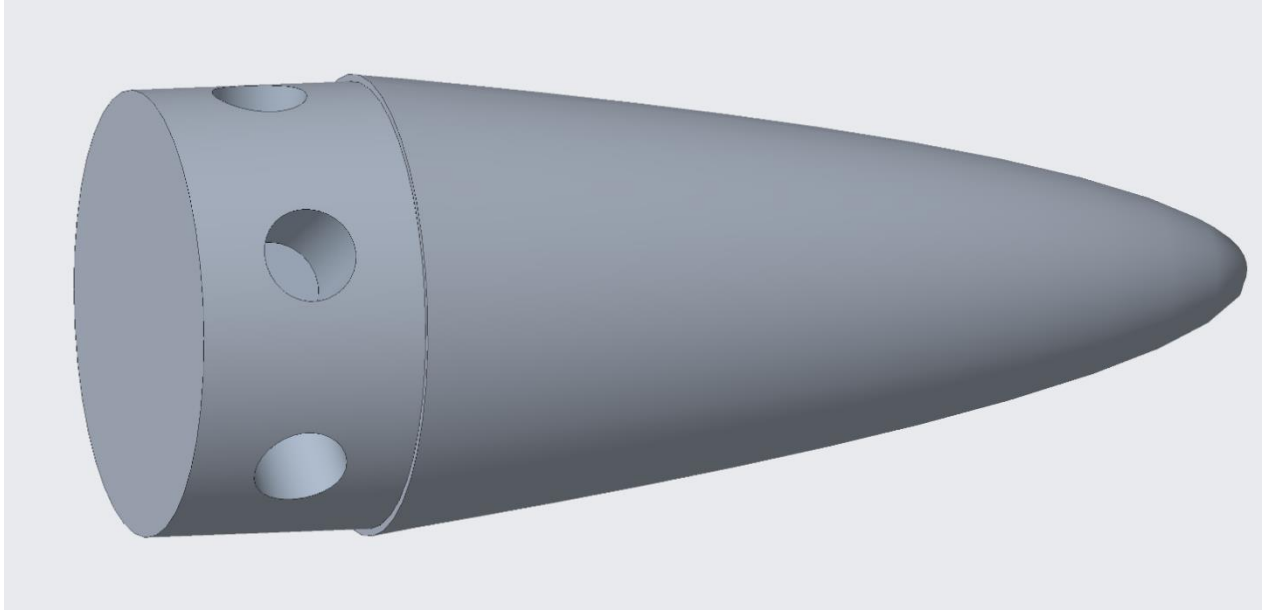


Figure 8. Nose Cone 3D Design

5.3 Wing Design and Wing Actuation

The wings will be our primary source of lift generation. The goal is to maximize the aspect ratio and the coefficient of lift. During the first stage of flight the wings must be housed inside the body of the projectile. Upon reaching the apogee of flight the wings will actuate, increasing the range of the projectile as well as gaining the ability to alter the flight path. The wing actuation system will follow the design of a three-bar linkage crank rocker mechanism. Both wings will sit parallel to one another inside the housing. In this position the front side of the wing will need to act as the outside of the projectile. Because of this the wing profile will follow the curve of the outer diameter of the outer shell. Each wing will be attached to a linear actuator. Upon receiving a signal, the actuators will push the slider forward forcing the pinned wing to rotate out of the shell. With the use of two different linear actuators it is possible to navigate the projectile with this simple mechanism. The actuator will be able to be drawn back to change the angle of one individual wing. This will result in the UAV turning. With a stroke of 50mm a maximum wing

span of 170mm can be obtained. It is important that the wing housing be isolated from the rest of the inner body of the projectile. They will each have a width of 25mm and a length of 90mm. When the wings are actuated there will be a slit in the side open to the air. This wing system will be a complete removable module to keep it isolated and allowing it to be an upgradable system for standard projectiles. This wing design will give us an aspect ratio equal to 3.6.

The wings will be machined out of 6061 general purpose aluminum in the University of the District of Columbia (UDC) machine shop. The slotting that holds the bar as well as the bar itself, will be additively manufactured by utilizing the EOS 3D printer at UDC. The material used will be 316L steel in order to achieve a higher strength and yield stress compared to aluminum.

5.4 Tail Design and Fin Actuation

The boat tail design can help reduce the overall drag on the projectile. For subsonic flow, the optimum boat tail is a gradual change in diameter [3]. This design gives the external airflow more time to adjust pressure and other flow conditions from the body tube to the boat tail. This shape will also allow us to develop fins that can be attached to the smallest diameter at the end of the tail. These fins will be instantaneously actuated upon launch, taking advantage of the airflow as an actuation mechanism. These fins will be folded down to be within the 50mm diameter. When fired they will extend past that constraint providing lift and minimal drag for the first stage of flight.

The tail will be machined out of 6061 general purpose aluminum in the University of the District of Columbia machine shop. It will extend past the base of the tail by 25mm in order to make a secure connection to the body. Threaded inserts will be attached to this extension. The fins will be pinned to the end of the tail with the freedom to be actuated by the force of the airflow. Each of the 6 fins will be machined from 6061 general purpose aluminum in the University of the District of Columbia machine shop.

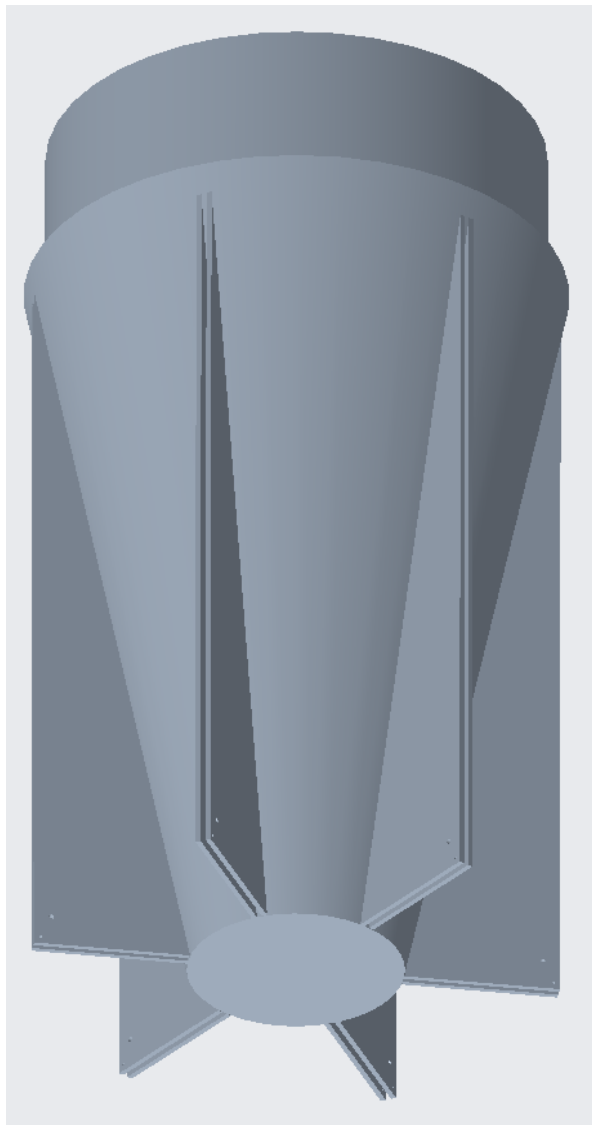


Figure 9. Tail 3D Design

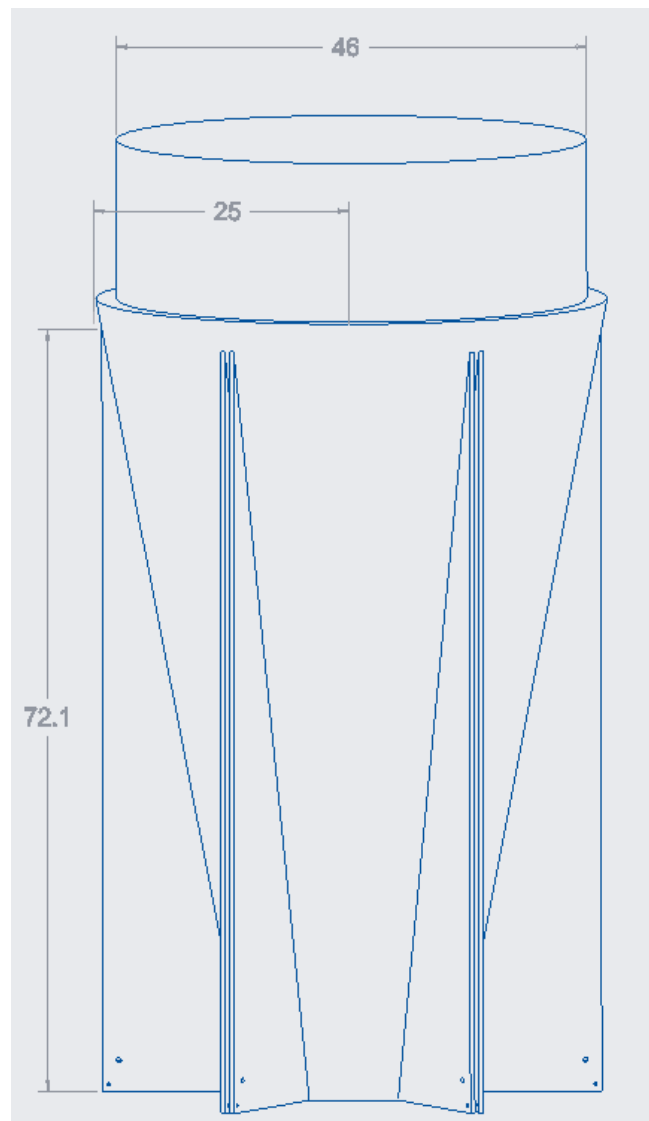


Figure 10. Tail Dimension Design

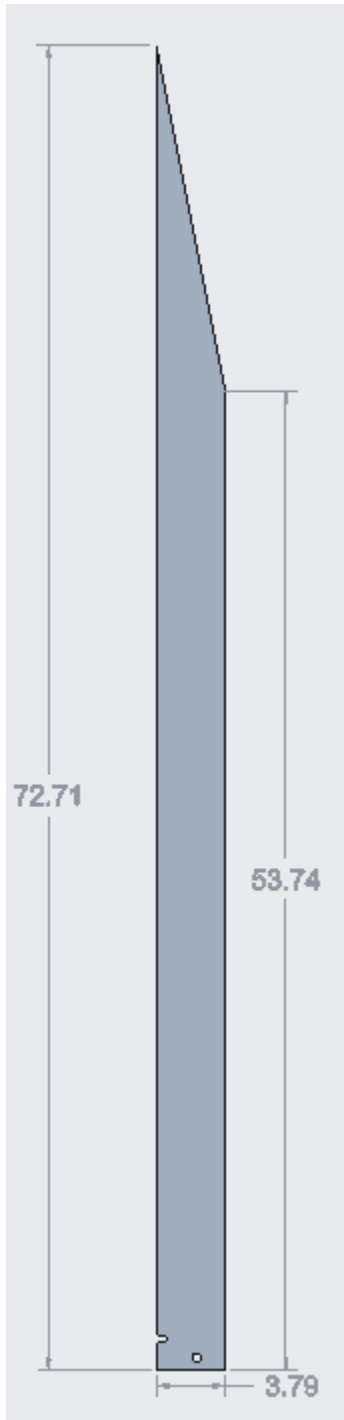


Figure 11. Fin Dimension Design1
(prototype)

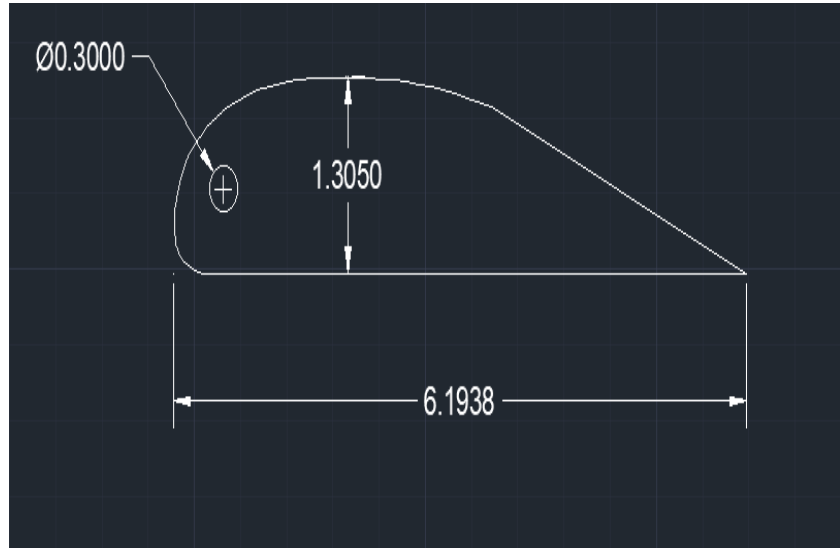


Figure 12. Fin Dimension Design2
(finale)

5.5 Aerodynamic Equations

With the set of requirements already defined we can advance to making preliminary calculations of the aerodynamic forces to confirm design feasibility. Using excel we calculated the standard equations for lift and drag as well as the maximum roll angle and turning radius [1]. The equations used are as follows:

$$5.2 \quad L = C_L \frac{1}{2} \rho A_{ref} V_{\infty}^2$$

$$5.3 \quad D = C_D \frac{1}{2} \rho A_{ref} V_{\infty}^2$$

$$5.4 \quad C_D = C_{D (profile)} + C_{D (induced)}$$

$$5.5 \quad C_{D (induced)} = \frac{C_L^2}{\pi (AR) e}$$

$$5.6 \quad D_{(skin \ friction)} = \left(\frac{1.33}{\sqrt{Re}} \right) \frac{1}{2} \rho A_{wetted} V_{\infty}^2$$

$$5.7 \quad \phi_{max} = \cos^{-1} \left(\frac{2mg}{C_{L-max} \rho A V_{\infty}^2} \right)$$

$$5.8 \quad R_{min} = \frac{m}{C_{L-max} \rho A \sin(\phi_{max})}$$

$$5.9 \quad AR = \frac{span^2}{area}$$

Where ρ = atmospheric density, A_{ref} = wing area, A_{wetted} = total surface area, V_{∞} = indicated airspeed, AR = aspect ratio of wing, Re = Reynolds number, ϕ_{max} = maximum roll angle, and e = span efficiency factor.

These equations were used with the proposed configurations and assumptions in order to calculate the aerodynamic forces. The results of these calculations can be found in the following section.

5.6 Results

	Mass (kg)	Cd	Cl	Re
	1.5	0.3	0.8	2743866.521
			mu (kg/m-s)	rho(kg/m³)
Lift (N)	272.61052		0.00001825	1.204
Drag (N)	126.51199		Aref (m²)	Awetted (m²)
Cd induced	0.0707714		0.073832	0.045
C	0.3707714		Vindicated (m/s)	AR
D(skin friction)	0.1667595		87.56	3.6
phi(max)	1.516792		e	
R (m)	0.106517		0.8	

Table 1. Aerodynamic Analysis Calculation Result Table

With these values calculated it seems that our preliminary design is feasible as it will produce enough of a lift to drag (L/D) to cross into the gliding regime upon wing actuation. It is important to note that due to the simplicity of the equations the lift and drag induced by the tail fins were neglected. Since the tail fins are lift generating components our lift to drag ratio should actually be larger than these calculated values. The fins will contribute to the drag force as well, however, they will provide more lift than drag subsequently helping us achieve a higher L/D ratio. We also used the maximum weight for these calculations. Further simulation will provide us with a better understanding of our assumed values. However, these calculations prompt us to move forward with our presumed design.

In attempt to verify the results and gain further insights we employed the help of Aerolab Rocket Drag and Stability Calculator. With the use of this software we were able to add the anticipated weight of each component and resolve the estimated center of pressure and center of gravity. We also verified the coefficient of drag that we used in the initial calculations.

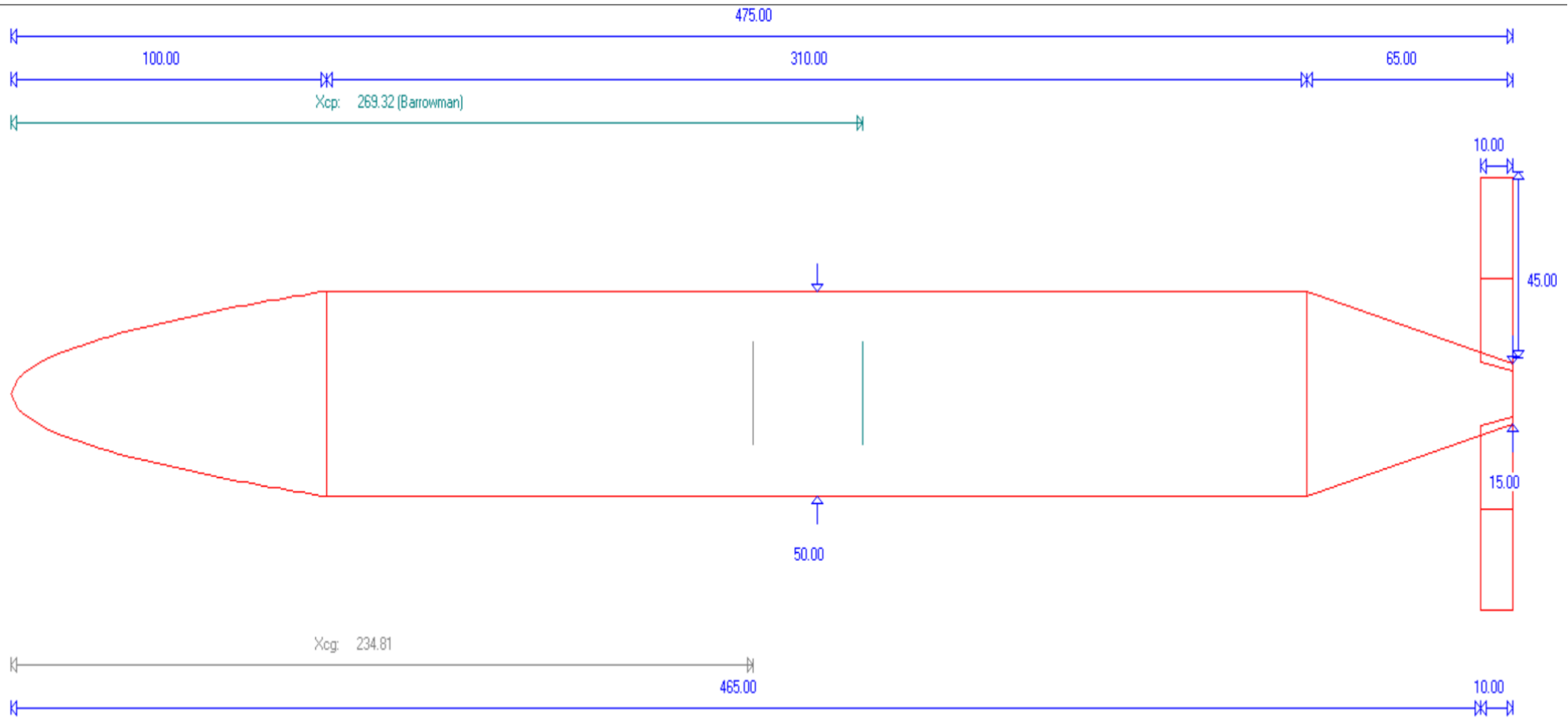


Figure 13. Center of gravity and pressure

Barrowman Center of Pressure: 269.31946
 Barrowman Cna: 3.930038
 Center of gravity (full): 234.808405

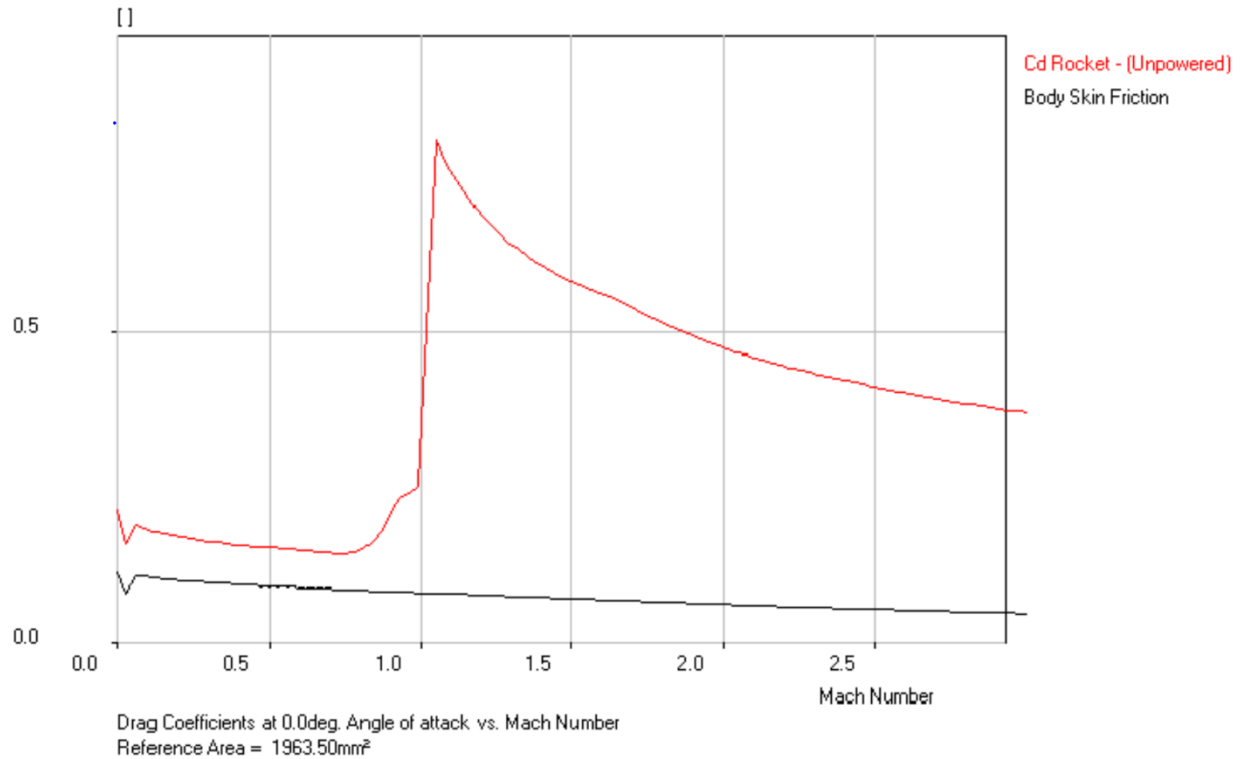


Figure 14. Coefficient of Drag Vs. Ma

The values produced from this simulation are in line with the values that were obtained through the equation. In order to find the center of gravity, there were input values of the estimated weight of the wings, actuators, batteries, payload, and a solid nose cone. The center of pressure is where the lift and drag force can be resolved for a free body diagram [1]. The location of these points is satisfactory for standard projectile design.

5.7 Trajectory

In attempt to confirm the design will carry the projectile the appropriate distance based on the previously calculated values, a computer program was created and employed. The trajectory chart was implemented using Python 3.7. There are multiple different flight paths that are analyzed. The first is without any actuation occurring (fin and wing actuation) simulating a

standard projectile. This results in a parabolic curve subjected to drag forces. It follows the kinematic equations for projectile motion. The next is when just the fins are actuated. This addition of lift with minimal drag results in a slightly further range and higher maximum height. It is assumed that the fins are actuated instantaneously. The final line indicates the path once the wings are actuated from the apex of the parabola. The wings provide a substantial addition of lift that successfully converts the flight path from projectile motion to gliding motion. The gliding motion equations [10] used are as follows:

$$5.10 \quad \dot{V} = -\frac{D}{m} - g * \sin\gamma$$

$$5.11 \quad \dot{\gamma} = \frac{L - mg \cos\gamma}{mV}$$

$$5.12 \quad \dot{H} = V * \sin\gamma$$

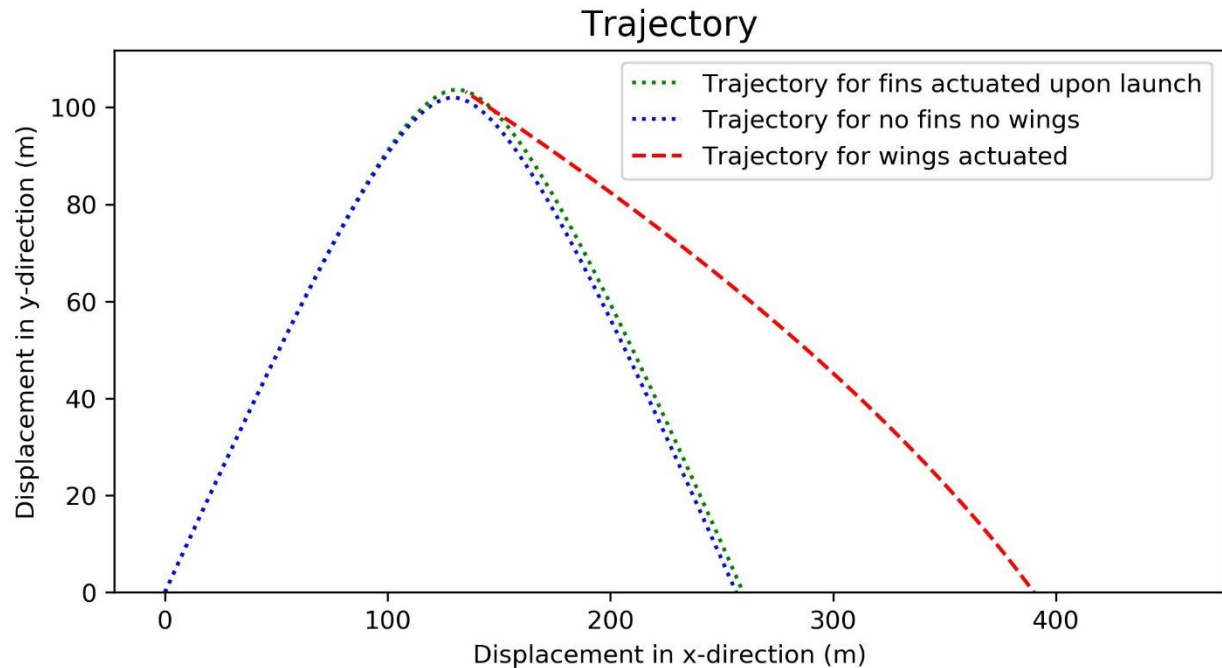
$$5.13 \quad \dot{R} = V * \cos\gamma$$

Where \dot{V} = the aerodynamic velocity with respect to time

$\dot{\gamma}$ = the angle between ground level and projectile trajectory

H = Height and R = Range

The gliding trajectory was used with the initial conditions of maximum height and half the range of the trajectory for the fins being actuated. Also, the initial velocity used was the velocity that was calculated at that point in the air of maximum height. It is also assumed that the wings are actuated instantaneously and done so when gamma initially equals zero.



6. Simulation Procedure

The design stage of the projectile as of now has a clear modeling concept, aerodynamic calculations, and a simple mechanical mechanism to actuate the wings. Using computer simulation software for multiphysics systems can be run anywhere because it is independent of the environment and can even be simulated on a microscopically scale. Simulation for the projectile will also help to identify the loads early on which can help to better optimize the design. Additionally, the simulation procedure for this project can aid on verifying aerodynamic calculations, the airflow pressure distributions, and it ensures early on the functionality of the design.

The simulation procedure will utilize the Multiphysics COMSOL software, which is designed to provide the most accurate results by minimizing the assumptions users must make.

With the aid of COMSOL Multiphysics software, finding the moments, stress, and forces that are exerted on the projectile becomes simple. The simulation on the projectile will have two stages for the procedure. The reasoning for the two stages is because the forces will act contrarily on the projectile during takeoff up until the apogee and after the apogee. The first stage of the simulation is to find all the forces acting upon the projectile from launch up until it hits the apogee. The second stage of the simulation will begin at the start of the apogee to the designated point. The apogee is when the wings will be actuated, and this stage has forces that differ from the first stage of simulation. The simulation will also use a modular based design. This means that every system of the UAV will be broken down into smaller parts called “modules.” The use of the modular design allows components to be easily replaced and allow integration of additional features. Once we can confirm are measured values through simulation, we will begin the fabrication for the wind tunnel testing.

A 2-Dimensional profile of the projectile with a laminar, turbulent, and transient state study was adequate to conduct this simulation. Drawing the power series nose profile was simply inputting the equation $y = R \left(\frac{x}{L}\right)^n$ into a parametric curve with the addition of lines for the body and tail of the projectile. To simulate a wind tunnel, a geometry of a semicircle and square was placed around the projectile profile. A material of air was then added to the domain around the projectiles profile. Next, an inlet and outlet were added to the domain of air surrounding the projectile profile, which was to mimic the wind tunnel testing. A fine mesh was also supplementary to the air domain, and projectile profile. Adding the mesh breaks up the model into smaller structural elements and each piece can be analyzed with the software. Finally, the simulation was ready to compute, and the results are shown below [3].

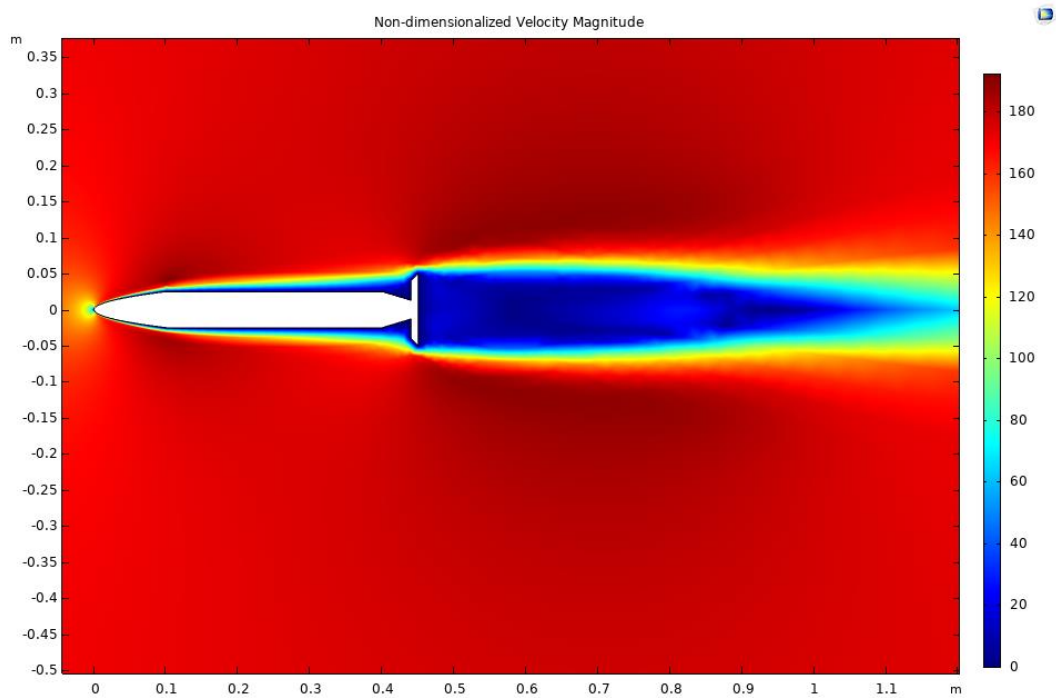


Figure 15. Velocity Distribution

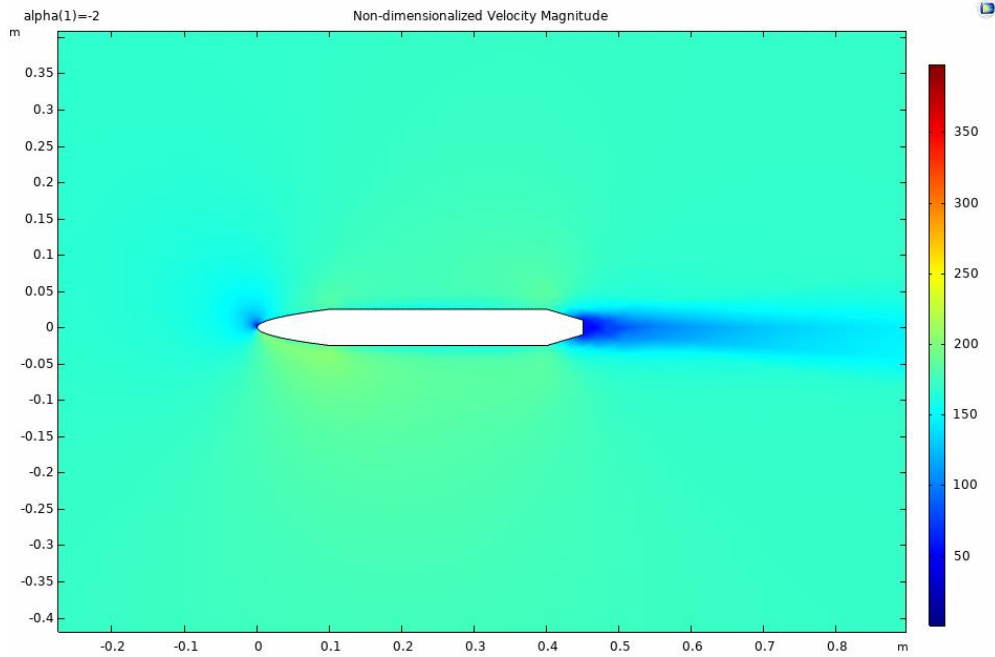


Figure 16. Velocity Distribution AoA=-2

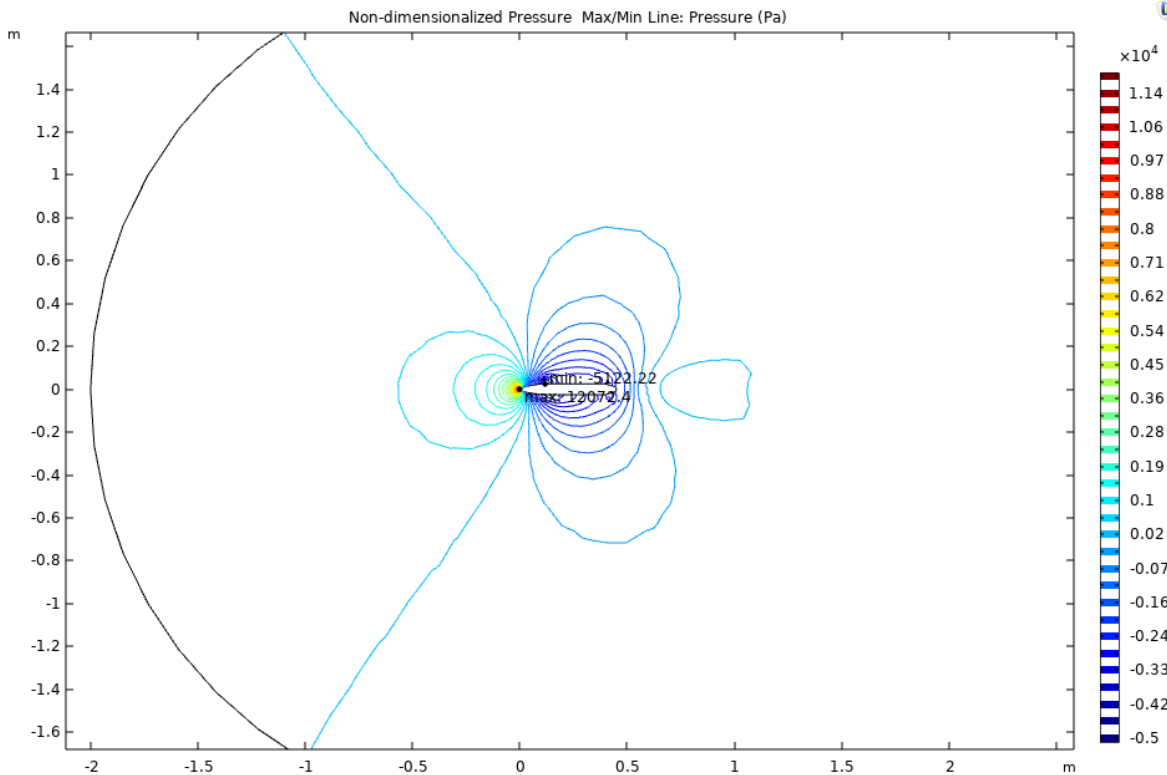


Figure 17. Pressure Distribution

As one can see from the results, the pressure distributions around the profile appears to be evenly distributed with the various angle off attacks. The highest pressure is at the nose of the projectile and then evens out around the profile. Also, a parametric sweep for an angle of attack was used in this study to simulate the pressure distributions at various angles. A parametric sweep is a function that allows the user to change the parameter values through a certain range [3]. Therefore, instead of manually changing property values and determining each one every time, you can just use the parametric sweep. For each angle of attack, the flow field surrounding the projectile will change.

The simulation results also showed that the velocity distribution around the tail of the projectile was insufficient. From figure 15, the velocity distribution around the fins are approximately 25 m/s. The original fin design was supposed to utilize airflow as a mechanism for actuation beginning from launch. Based off the data collected from the simulation, the velocity profile surrounding the fins is inadequate for actuation. Therefore, a new strategy using a spring-loaded mechanism was devised in order to achieve the proper actuation of the fins.

7. Manufacturing of Components

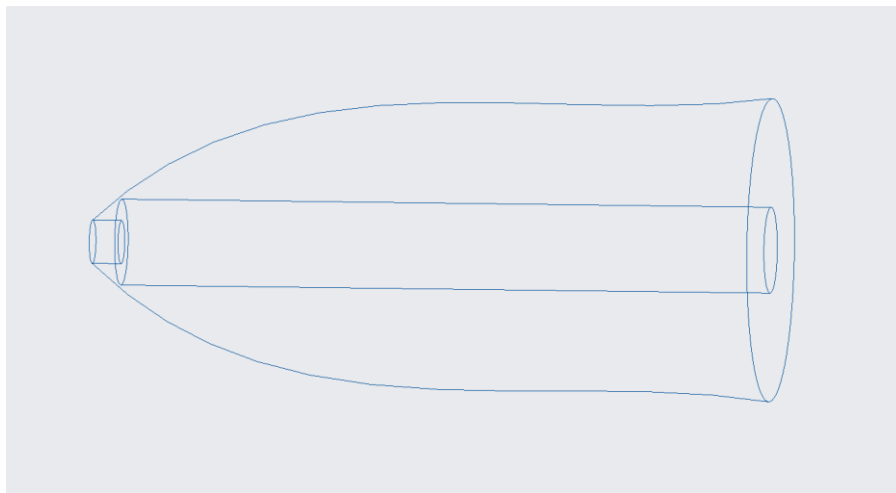
In compliance with the University of the District of Columbia's Small Business Enterprise policy, the parts were obtained from WS Jenks, a local small business in NE DC. The order consisted of two feet of a general purpose aluminum solid rod with an outer diameter of two inches, two feet of a general purpose aluminum hollow tube with an outer diameter of two inches and a thickness of 0.065 inches, and a 2 x 1.025 aluminum sheet.

7.1 Nose cone

The nose cone was manufactured from the solid aluminum rod. The first step was cutting off the appropriate amount with a band saw. The total length of the nose cone is 125 mm with the 25 mm attachment piece included. Using the band saw 140 mm were removed in order to provide enough space for the metal to be gripped in the laith machine. The lathe machine was used to remove material from the aluminum bar in the UDC machine shop. The lathe machine works by rotating the piece and bringing a tool into contact. The cutting tool, high speed steel, is fed into the workpiece for a desired depth and in the desired direction. Since the cone is of a parabolic shape the formula used to generate the design was also used in the manufacturing process. Using the formula $y = R \left(\frac{x}{L}\right)^n$ where $n = 0.5$; we were able to calculate how far in the tool should be forced into the workpiece for every centimeter traveled along the x-axis. This resulted in our desired shape. After the desired shape was created it was sanded down in order to achieve a smooth and uniform finish. Then the tip was inserted into the chuck and 0.065 inches worth of material were removed for 25 mm from the base of the cone so that the cone could be inserted into the housing body.



The design calls for a camera to be able to be mounted at the front of the nose cone. The camera that was purchased has two different diameters that need to be hollowed out from within the solid cone that was created with the laith machine (figure below).



To achieve the internal features two different diameter screws were needed. The first screw used was that of the same diameter as the camera lens and was drilled from the front of the nose cone. The second, and wider, hole was drilled into the back. Because of limitations in equipment at the UDC machine shop, we were unable to drill the entire distance with the required drill bit. We went

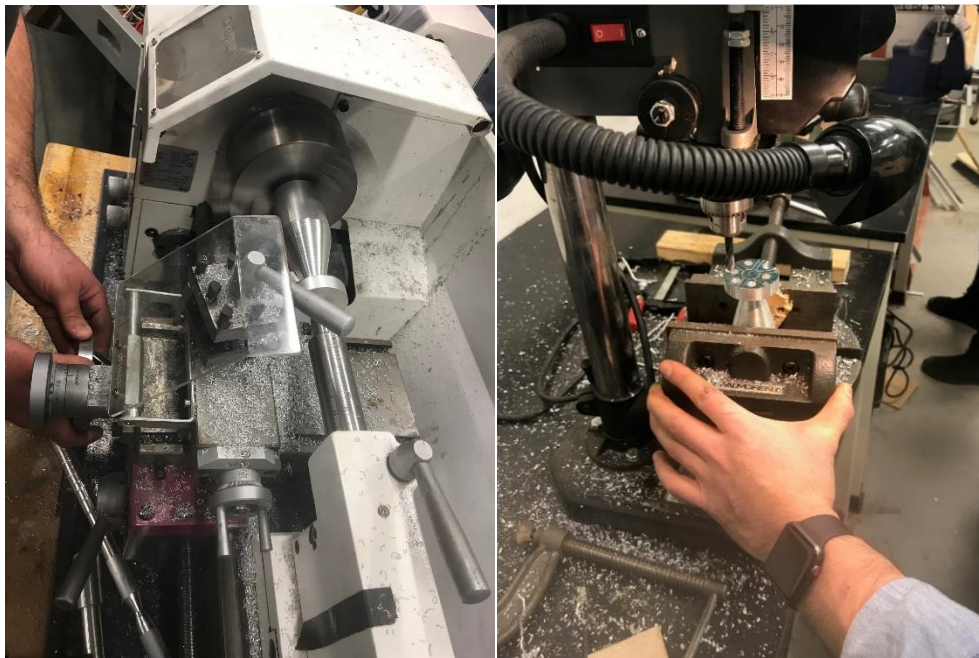
about 75 mm of the required 120 mm. The final way was done manually with a power drill. This was a slow and arduous process. With much patience and a steady hand, the desired shape was created. The shape also the camera to be inserted into the back. It is limited in its degrees of freedom in every direction except for coming back out the back from which it is inserted. In order to address this issue, the TAZ LULZBUT was utilized to print out an insert. This insert holds the camera from the back making alignment easier and also prevents the camera from moving back out from the cone. The insert is hollow which allows for the wires to be flowed back through to the body of the projectile. With the insert in place the camera is now unable to move in any direction and is firmly attached in its proper place (figure below).



7.2 Tail and Tail Fins

The tail and tail fins are an intricate design that require multiple machining techniques. We began with the 2" solid rod and cut out 100 mm to work with. The rod was then placed within the chuck of the lathe to begin the machining process. We brought the tool into the work piece to achieve the desired taper, leaving the area that would be the fin holders untouched (figure below). Upon achieving the desired taper, the piece was sanded down. The piece was then flipped around, and we removed 0.065 inches for 25 mm at the base. Like the nosecone, this was to be able to fit into the body housing where it could be attached with screws.

To machine the wing holder region the milling tool was used. Milling is a process performed with a machine where the tool rotates to remove the material from the work piece present in the direction of the angle with the tool axis. The workpiece is held on the worktable of



the machine. The table movement controls the feed of workpiece against the rotating cutter. The cutter is mounted on a spindle or arbor and revolves at high speed. Except for rotation the cutter

has no other motion. As the workpiece advances, the cutter teeth remove the metal from the surface of workpiece and the desired shape is produced [11]. The desired shape was drawn onto the back of the workpiece and then a combination of drilling and milling was used to remove the excess material. To get a smooth finish, a manual sanding was performed. The final step is making the slots in the fin holders where the fins are attached. This was a very tedious, arduous process. Because of the limitations on the tools available, this step had to be done manually with a grinded down blade from a handsaw. After many hours of skilled machining the slots were hollowed out satisfactorily.

The fins were manufactured from aluminum sheet metal. They were cut with a sheet metal cutter to a relatively similar shape as what was desired. They were then placed together and grinded down in order to achieve a uniform shape for each piece. The fins are attached to the back of the tail with a simple screw and bolt connection. A hole was drilled between all three sides and the screw tightened securely. With all six fins attached the manufacturing process of the tail is complete.

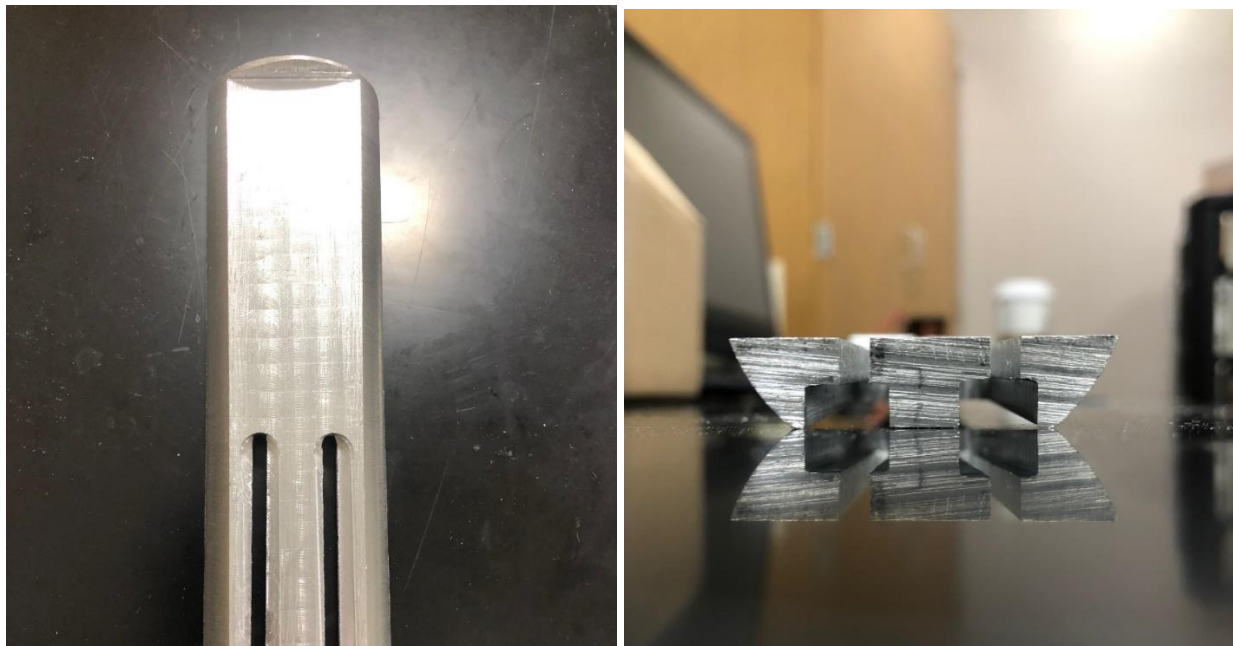
7.3 Wing System

The wing system consists of multiple components that all needed to be manufactured separately. The parts include two wings, a wing plate for the slider mechanism, and two bars that connect the slider to the wing. The wings and the wing plate were manufactured from aluminum while the wing bars, for this prototype, were additively manufactured using PLA at an 100% infill for maximum strength.

The wings were made from an aluminum bar that was 1” wide. The piece was cut into two identical pieces that were each 100mm long and 5mm thick. Each piece was then milled to remove

the material where the wing bar would sit and be allowed to move as the slider is pushed 50mm. After finishing the milling process holes were then drilled into the wings, one for attachment to the wing bar, and the other to be pinned down to the wing plate.

The wing plate was cut out from the aluminum solid rod that was also used for the nosecone and tail piece. After cutting out a middle portion with the band saw both sides of the plate were milled down in order to be made flat. This process involved a lot of material removal, and since the only available cutting tools were small it was a very slow process. Upon achieving two flat surfaces we were ready to then create the slots for the sliders. This was done with two different size milling tools. The slots were ideal for the slider as it slides smoothly without being able to move in the z direction.



We ultimately had to scrap our original idea of printing the wing bars out of 316L steel using a selective laser sintering process. Instead, we decided to use rapid prototyping with the

extrusion based TAZ LULZBOT available to us at UDC. These small bars were printed in 30 minutes with an infill of 100 percent to ensure the maximum strength available to us with this manufacturing process.

8. Electrical

8.1 System Requirements

Using the projectile objectives and requirements, the team performed prototype modeling to determine specific aerodynamic force and electronic requirements.

For the projectile to fulfill its intended purpose, we must have the following:

1. sensors that detect the projectile's position in the air
2. a camera or sensor that will provide live footage
3. a microcontroller that will use the data from the sensors to properly control the actuators
4. communication devices that will transmit position data and video footage to a ground system for analysis and storage

With these objectives in mind, we must employ a closed-loop feedback system for the projectile as there will be constant adjustment and error reduction in reaching the target. Because the projectile will be a mechatronics project, the electrical system will compose of sensors to gather critical information about the projectile, a controller to use and process that information, a communication system that will transmit video footage to a ground receiver and the actuators to receive the resulting control signals from the microcontroller. After the actuators perform the required action, the sensors will then detect any changes and again send information back to the microcontroller. The independent ground system will only store live video footage.

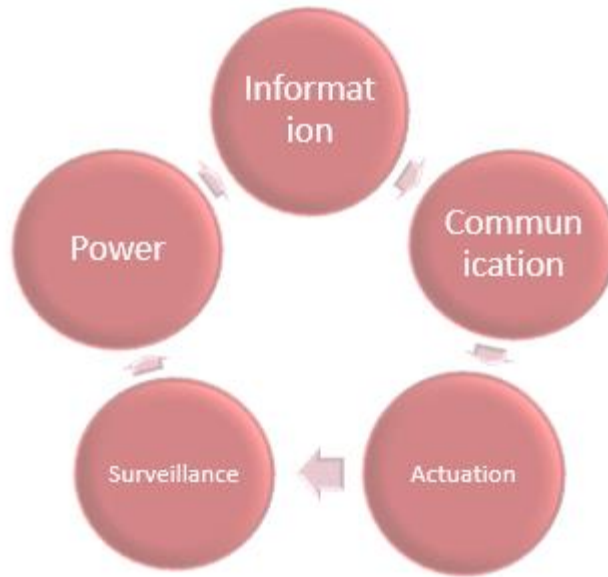


Figure 1: Figure 18. A general idea of the control system for the UAV.

8.2 Closed-loop Feedback System

In the first part of the feedback system, an Inertial Movement Unit (IMU) will be used for detecting the position of the projectile and will send that information to the microcontroller for processing. The camera that provides video footage will be independent of the control process as we only require live footage. From the IMU, we can gather the necessary variables to calculate and maximize lift at every point of launch. On the ground, video footage of the launch will be recorded and stored for future analysis. Using the information sent from the IMU, the microcontroller will then output the appropriate control signals to the actuators to achieve desired lift. This makes up the last parts of the feedback system. Whatever changes are made from the servos, the IMU will pick that up and restart the process again.

Because this is a feedback system, this makes the Arduino Micro the ideal microcontroller to use for this project as there are various applications we can use to program the microcontroller: Arduino IDE and Altair Embed. Arduino IDE allows us to write code line-by-line and program it to the Arduino board. However, Altair Embed allows us to create a block diagram that illustrates

the closed-loop feedback system that we need and then converts the diagram into programmable code onto the Arduino microcontroller. Five systems will be used to create a closed-loop feedback system.

8.2.1 Power System

The onboard avionics suits are based on the closed-loop system that will be powered by two 3.7-volt Li-Po batteries connected in series to create 7.4 volts. Other projectile components will only require 5 volts and ground provided by the microcontroller.

8.2.2 Surveillance System

The system gathers visual data from projectile and provides autonomous surveillance of defined perimeters and real time cueing to the ground system. This system will use a separate first-person view (FPV) 3MP camera with a built-in 5.8GHz transmitter to send footage to a ground system.

8.2.3 Information System

The system processes data from sensors and distributes them to the microcontroller. The microcontroller will be responsible for most of the information processing as they are both compatible with the 9-Axis Inertial Measurement Unit (IMU).

8.2.4 Communications System

Using the built-in 5.8GHz video transmitter in the separate camera and a 5.8GHz receiver compatible with Android devices, live footage of the launch will be provided and recorded.

8.2.5 Actuation System

The microcontroller will send control signals resulting from computed process using gathered information. Actuonix L16-R 50mm Miniature Linear Servos were chosen because linear actuators with 50mm stroke are required. In order to actuate release mechanisms and control surfaces, 54g Actuonix L16-R 50mm Miniature Linear Servos were chosen, based on form factor linear motion, and acceptable stroke lengths (50mm), force (200N), and speed (32mm/s). This unit is shown in Figure 19. The canard configuration utilized two servos, both for the wing actuation system, and both connected to each slider forward forcing the pinned, as shown below. The servos were air-gun tested in various orientations and determined to be G-tolerant to at least 3000 G, the maximum tested load.

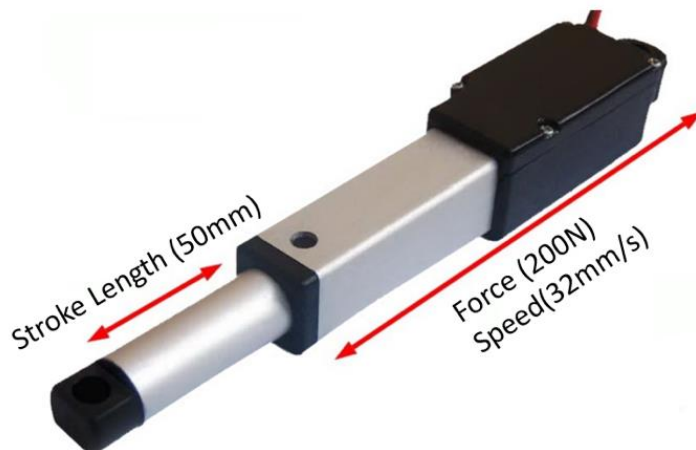


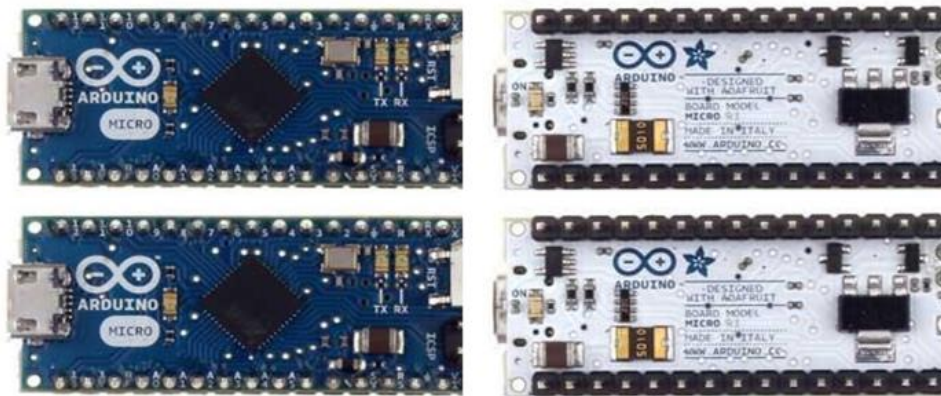
Figure 19. L16-R servo (68 mm L x 18 mm W x 20 mm)

8.3 Ground System

The system is a 5.8GHz receiver connected to a Galaxy Note 3 phone – which is UVC (USB video class) compatible. Current android phones will not work with the receiver as they do not have the UVC capability required. The 5.8GHz receiver has a range of between 200 – 400 meters and can record the launch as it progresses.

8.4 Arduino Micro

Because the electrical system of our projectile is responsible for gathering projectile position information, providing surveillance and controlling the actuators, a powerful microcontroller must be considered. Due to the size and weight constraints of the projectile, we have chosen the Arduino Micro microcontroller to gather data from smaller sensors and provide actuation due to its small size and ease of use.



NEW FIGURE: ARDUINO MICRO

9. Assembly & Testing of Components

Now that all of the electrical components have been grouped, see Sec. 8, and all of the individual parts of the projectile have been fabricated, Sec. 7, the time has now arrived to assemble all of the electrical system components to be housed within the projectile. We will start by describing how the projectile was assembled starting from the tail end and we will work our way within the body until the projectile is finally enclosed at the nose end. Within the projectiles' airframe, we will also go in depth in describing how the micro-electrical-mechanical-system (MEMS) was fixed within the cylindrical enclosure to be joined to the wing plate that actuates the wings in flight via 3-bar mechanism and built-in rail. The wing plate, now attached onto the linear actuators via linear actuator housing, is then affixed to the nose which is finally introduced into the airframe to be assembled into one single unit, the projectile.

9.1 Attachment of Spring-loaded Fins onto Tail End.

The fins are attached to the back of the tail with pop rivets. The rivets allowed for a tight, secure fit and perfect rotation starting from resting phase to spring-assisted fin deployment. Once the rivets secured the fins to the tail, a single screw was attached directly on the center of the machined tail end by means of drilling a pilot hole then tapping the pilot hole so that the single screw can be secured to the back end of the tail. The single center screw on the tail was used to act as an anchor to attach 6 springs that will assist in deploying the tail fins starting from their resting phase. The other ends of the springs were then fixed on the spine of the tail fins to allow for full rotation about an axis. With all six fins attached, as well as the springs, the assembly process of the tail is complete.

9.2 Attaching the Tail End of the Projectile to the Body

With the spring-loaded fin mechanism secured to the tail end of the projectile, it was now able to be fixed on to one side of the airframe, i.e. hollow cylindrical body. The tail of the projectile was machined so that it can be easily inserted into the airframe in a male-to-female connection. The outer perimeter of the tail was recessed to the exact same depth of what would be the thickness of the airframe. The airframe was easily sleeved onto the tailfin, were six pilot holes were drilled and then tapped so that six machine head screws affixed to body to the tail end of the projectile securely. The joining of the tail to body is now complete.

9.3 Fixing the wings onto the wing plate.

Because all the projectiles wing actuation and electrical system could not directly be fixed within the body, it was necessary to assemble the wings onto the wing plate. The wing mechanism assembly had to also be attached to the actuator housing since the 3-bar mechanism needed to be in-line with the linear actuators. The Wing and Actuator assembly, once joined, would be fixed onto the base of the projectiles nose cone with two screws. Attaching the wings to the wing plate required that the shoulders both wings be fixed to the wing plate with a pop rivet. The rivet allowed the wing to rotate about an axis while also maintaining a secure anchor to the wing plate. One end of the linking bars was then riveted onto the wing to allow rotation, while the other end of the linking bar was secured to the rail of the wing plate using a nut and bolt. The nut and bolt system allowed for the head of the bolt to freely slide along the underside of the rail whereas the nut sandwiched both the arm of the actuator onto the other end of the additively manufactured bar.

This connection perfectly mated the wing plate and the actuation housing in parallel with linear actuator arms and linking bar. The Wing and Actuator assembly is now complete.

9.4 Assembling the Camera and Camera housing within the Nose Cone

Before the Wing and Actuator assembly can be securely attached onto the nose cone, the camera in its housing had to be securely inserted within the nose cone. The camera attaches to the tip of the housing which allowed it to be easily inserted with in the nose cone by simply sliding the camera housing into the base of the nose cone. On the tip of the nose cone was the camera itself, were a recessed hole made at the tip of the nose cone allowed the camera to rest upon such hole. Let's continue with the assembly of the wing and actuator mechanism onto the base of the nose cone.

9.5 Attaching the Wing and Actuator assembly onto the nose cone.

Two pilot holes were drilled into the base of the nose cone, and later tapped, so that the head of the wing plate assembly could be attached using 2 machined flat head screws. Two horizontal slots were made at the head of the wing plate for easy adjustment in order to finally mate the nose, wing, actuator assembly into the slotted, open end of the airframe. Once the triple assembly has been secured, it can now be inserted with in the airframe for final configuration.

9.6 Inserting the triple assembly with airframe.

Where the wing and actuator assembly mated to the nose cone, the base of the nose cone was also machined in such a fashion where the outer perimeter base of the nose cone could be easily inserted into the airframe, male-to-female fashion connection. Similar to how the tail of the projectile was secured onto the airframe, by 6 machine screws, the slots on the airframe guided the wings on the triple assembly neatly into place. The wings are now free to actuate within the air

frame and deploy to their full extended programmed position that allows for guided flight. The assembly of the entire projectile is now complete.

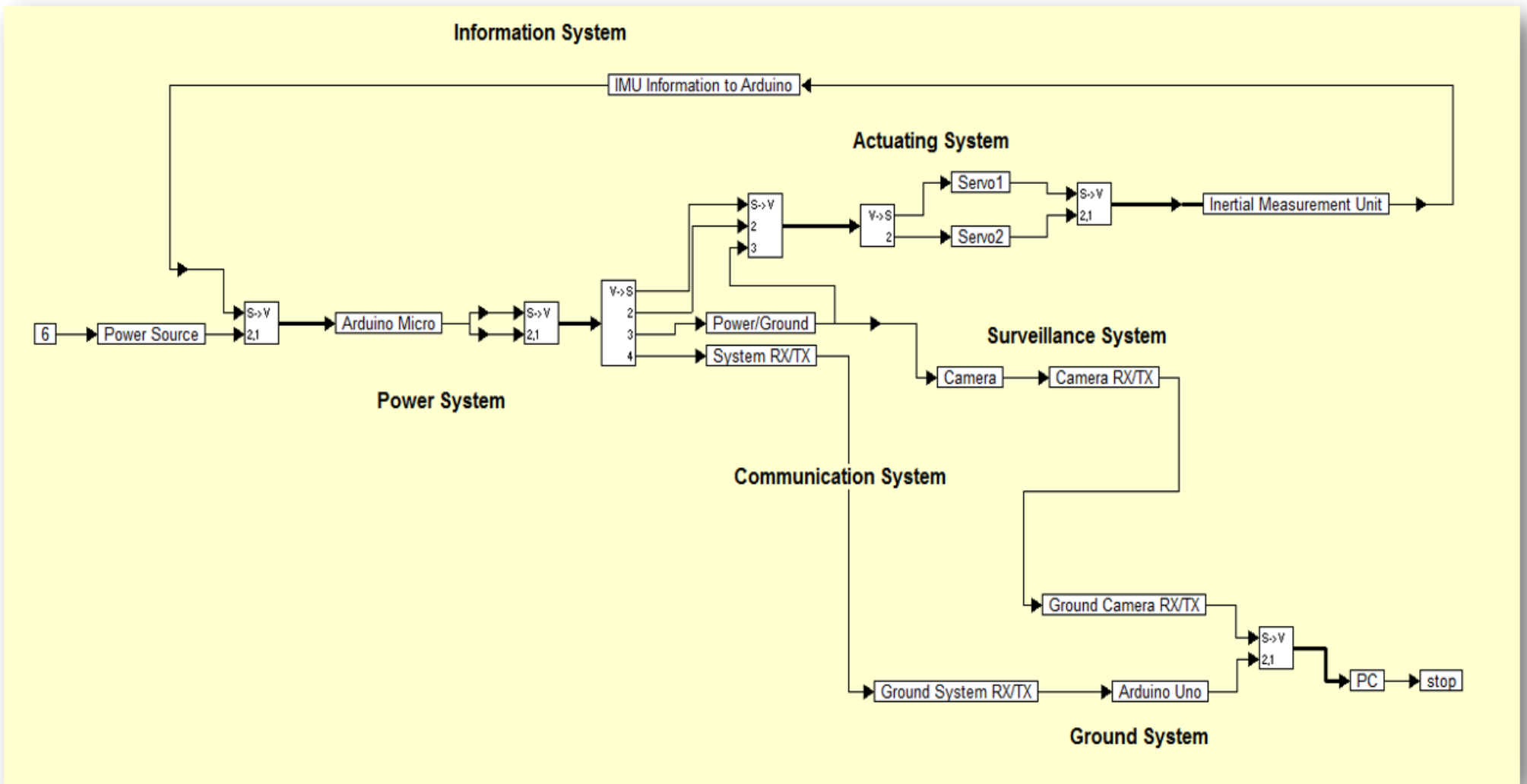
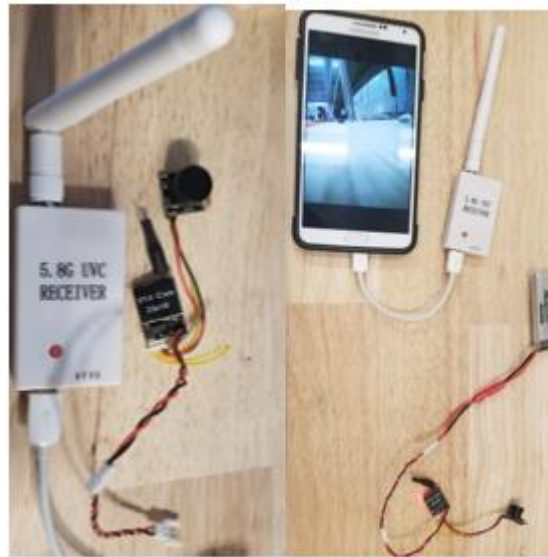
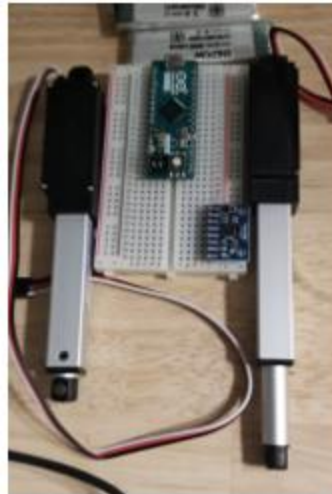


Figure 23 Electrical system flow chart

In order to meet our goal of a true mechatronics design in our projectile, we must employ wing actuation by way of the linear servos. The microcontroller will be using pitch information from the IMU (Arduino-compatible GY-521 module) in order to control the servos. A 5.8Ghz camera transmission system powered by its own battery will provide surveillance during launch while a ground receiver connected to an Android phone will capture the video. The projectile circuit will be powered by 2 3.7-volt Li-Po drone batteries – putting these batteries in series will provide the microcontroller 7.4 volts while the other components only require 5 volts directly from the microcontroller.

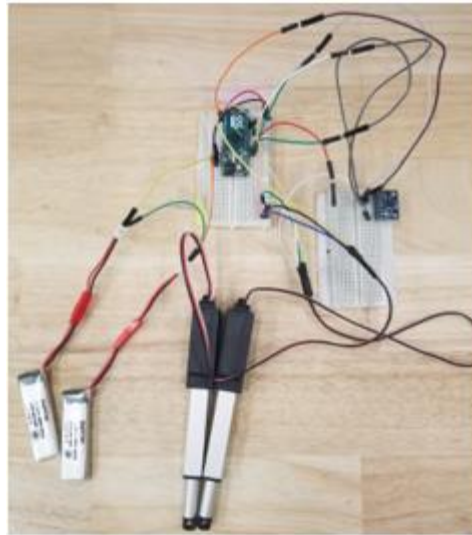


NEW FIGURE: Working camera system with live footage.



NEW FIGURE: Components used in the actuation and information systems.

While putting together the circuit, a number of challenges were met. These challenges were issues with powering, compatibility, coding and transmission. When first assembling the circuit, I have learned that coin cell batteries did not provide enough power to the microcontroller. As a result, Li-Po batteries were used as an alternative. Once power was established, there was difficulty getting the IMU to interact with the servos through code. This was in part due to lack of knowledge about proper coding of the IMU in order to obtain pitch, yaw and roll. Many different methods of coding failed, but I was eventually required to learn more about the IMU's digital architecture to properly code it. It was then I was able to achieve pitch, yaw and roll – but still could not establish a working interaction between the servos and the IMU. It was then discovered that there was an optimization issue with the code, requiring me to restructure it. Once resolved, the servos were controlled by the pitch data.

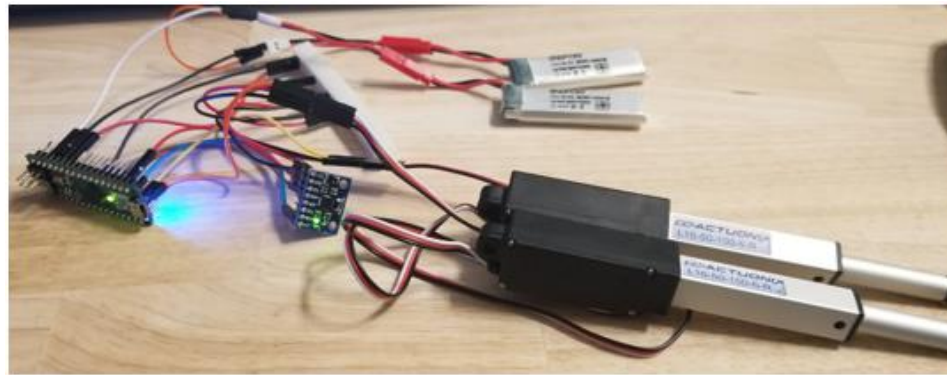


NEW FIGURE: Breadboard prototype of circuit used for testing.

Once the circuit was assembled, we could then perform a variety of tests to assess any problems. The first test was the surveillance system and assessing its distance and transmission ability through the aluminum body of the projectile. The next round of tests involves the projectile circuit as longevity and durability must be assessed. These tests were performed to get an idea of the limitations of the electrical system.

Results

After testing the range, we could only see live footage up to around 350 ft (>100 m) away from the camera without any disturbance. This distance was slightly less once the camera was placed in the nosecone. Using a 5.8GHz system wasn't ideal as the signals will not travel very far, but this camera system was the best choice given the constraints.



NEW FIGURE: Final implementation of the projectile circuit.

Although we didn't excel with the camera system, we have exceeded expectations with the projectile circuit as battery life was far longer than anticipated. The launch will last anywhere between 2 to 5 minutes, so we require the system to be powered for at least 10 minutes. After testing, we have discovered that the projectile circuit lasts up to 7.5 hours on battery. Moreover, the camera can last up to 1.25 hours on battery while the ground receiver will last 35 minutes on the phone's battery. Concerning cost, the electrical system only cost us \$218 from the \$500 budget with the servos being the most expensive. All of these results have exceeded anything we have expected from the system.



NEW FIGURE: Electrical system weighed on a scale.

9. Hybrid Projectile Bill of Materials (BOM)

Assembly Name : Mechanical & Electrical
Components & Telemetry




Assembly Revision : 1st






Approval Date : Nov. 7, 2018

Part Count : 56

Total Cost : \$1,307.43

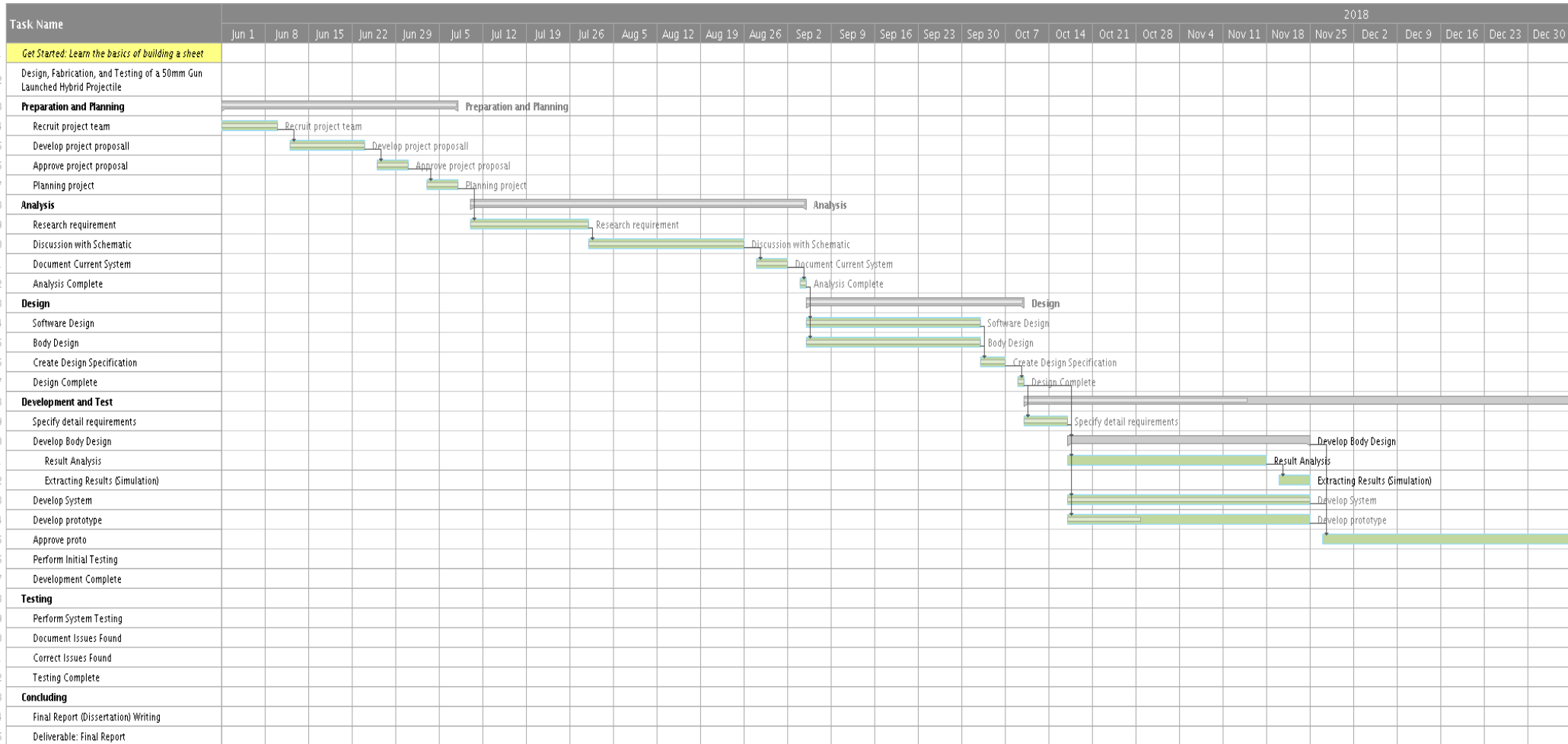
Part #	Part Name	Description	Qty	Units	Picture	Unit Cost	Cost
A000053	Arduino Micro	Micro-Controller	6	Each		\$19.80	\$ 118.80
A000066	Arduino Uno	Micro-Controller	2	Each		\$22.00	\$ 44.00
380	3 Volt Lithium Coin Cell Battery	CR1220 12mm Diameter Lithium Coin Cell Battery to Power Components	12	Each		\$0.95	\$ 11.40
WGDC 1	WGCD 433 MHz RF Tx & Rx for Arduino	Tx/Rx Communication	2	Each		\$10.55	\$ 21.10
3133	Adafruit Ultimate GPS Featherwing	Tx/Rx Communication	2	Each		\$39.95	\$ 79.90
S9-Block	Extra Slide Block for Micro Linear Slide Rail	Ball Bearing Slide Rail Carriage	4	Each		\$20.00	\$ 80.00
Indicator	Actuonix Actuator Position Indicator	Visual Feedback for Actuators	4	Each		\$20.00	\$ 80.00
S9-50	Actuonix Micro Linear Slide Rail	Linear Slide Rails 50mm	4	Each		\$40.00	\$ 160.00
L16-R	Actuonix L16-R 50mm Miniature Linear Actuator	Linear Servos for Arduino 63:1 6 - vdc	4	Each		\$70.00	\$ 280.00
1232055	Sunkee 10-DOF 9 - axis	Inertia Movement Sensor	2	Each		\$26.35	\$ 52.70

1604	Adafruit 10-DOF IMV Breakout	Inertia Movement Sensor	2	Each		\$24.72	\$ 49.44
1181449	Small 120 Degree Camera	Camera	2	Each		\$19.99	\$ 39.98
Turbo SDR2	Turbo Micro SDR2 1/2.8 2.1mm Camera	Camera	2	Each		\$35.99	\$ 71.98

Part #	Part Name	Description	Qty	Units	Picture	Unit Cost	Cost
89965K841	3 feet General Purpose Aluminum Tubing 2" OD 0.065" thickness	Body of projectile	1	Each		\$39.84	\$ 39.84
88615K58	3 feet Formable Easy-to-Machine 2011 Aluminum Rod	Wings, nose, tail	1	Each		\$86.71	\$ 86.71
91732A202	18-8 Stainless Steel Helical Insert, 2-56 Right-Hand Thread. 0.125" Long (10 pack)	Connections for body and tail	2	Each		\$3.89	\$ 7.78
422B-55ML	422B - SILICONE MODIFIED CONFORMAL COATING	Conformal Coating for PCB	2	Each		\$12.95	\$ 25.90
3037000	Shock Absorbing Sorbothane	Sorbothane is a proprietary, visco-elastic Polymer	2	Each		\$28.95	\$ 57.90
Total			56				\$ 1,307.43

10 Gantt Chart

10.1 Fall Semester



9.2 Winter Semester

Task Name	Jan 6	Jan 13	Jan 20	Jan 27	Feb 3	Feb 10	Feb 17	Feb 24	Mar 1	Mar 8	Mar 15	Mar 22	Mar 29	Apr 5	Apr 12	Apr 19	Apr 26	May 3	May 10	May 17	
1 <i>Get Started: Learn the basics of building a sheet</i>																					
2 Design, Fabrication, and Testing of a 50mm Gun Launched Hybrid Projectile																					
3 Preparation and Planning																					
4 Recruit project team																					
5 Develop project proposal																					
6 Approve project proposal																					
7 Planning project																					
8 Analysis																					
9 Research requirement																					
10 Discussion with Schematic																					
11 Document Current System																					
12 Analysis Complete																					
13 Design																					
14 Software Design																					
15 Body Design																					
16 Create Design Specification																					
17 Design Complete																					
18 Development and Test	Development and Test																				
19 Specify detail requirements																					
20 Develop Body Design																					
21 Result Analysis																					
22 Extracting Results (Simulation)																					
23 Develop System																					
24 Develop prototype																					
25 Approve proto																					
26 Perform Initial Testing																					
27 Development Complete																					
28 Testing																					
29 Perform System Testing																					
30 Document Issues Found																					
31 Correct Issues Found																					
32 Testing Complete																					
33 Concluding																					
34 Final Report (Dissertation) Writing																					
35 Deliverable: Final Report																					

11. Future work

The ultimate goal of this project is to fabricate and test a physical projectile. The spring semester for the projectile had a monumental task for the manufacturing process. The process was done entirely through traditional techniques using the lathe machine, milling, cutting, and drilling. The power series nose for the projectile was created using the lathe machine, although to make a shape using the equation $y = R \left(\frac{x}{L}\right)^n$ was unfeasible. Therefore, its best to use the CNS in the future for better accuracy and precision. The tail and fins of the projectile were also a challenge to fabricate without the aid of a CNS machine, which can also be improved in the forthcoming. The fins of the projectile may have been the most challenging part of the process because of the limitations in the machine shop. The material of aluminum that was to be removed for fin actuation was tremendously difficult. Upcoming senior groups will need an advanced additive manufacturing technique in order to properly design fin actuation. A spring-loaded mechanism was also used for fin actuation, although further improvements can also be made for an optimal design.

The wing system was designed to fit inside the body of the projectile with a narrow-slit running along the side body. This narrow opening on the body was cut for when the wings are extended at the apogee of flight. One dilemma for the wing system was that during the extension of the wings, there would still be a small opening with the extension of the wings. Additional improvements need to be made on closing this region of space because this will alter the aerodynamics for the projectile. The last object to improve the wing actuation system is the slider mechanism. The original plan was to use the EOS laser sintering 3-D printer to manufacture the

steel bar. However, due to the limitations of the machinery we decided to 3-D print the bar using plastic.

The testing of the projectile was one part of the project that we didn't get to because of the limitations on the project. A wind tunnel test for the projectile would be needed in the future to ensure the calculations and simulations are correct. Another part of the testing would have been on the actual launching of the projectile. This also was not possible for our group because of strict governmental security clearances. The internal designs for housing the electrical components also needs improvements on proper housings in order to prevent vibrations and reducing G-forces onto the projectile. Lastly, the code to engage the actuators need improvements as well. The actuators need to be able to extend individually to achieve the most sufficient flight paths.

Upon discovering that the electrical system fell well within the constraints while providing wing actuation, there was much room for improvement. Providing wing actuation by way of the electrical system was only our first step into transforming this projectile into a true mechatronics project. One of the things we must do in the future is to display critical information on the ground receiver screen. Real-time information such as time, location and positional data must be transmitted through the microcontroller, then onto the screen. Secondly, we must be able to control the projectile from the ground. This will require an enhanced, long-range communication system. Lastly, we must have a way to store real-time information for later analysis. Once these tasks are completed, we can then test out a Raspberry-Pi based system with object-detection capabilities.

12. Appendix

Trajectory code:

```
import numpy as np
import matplotlib.pyplot as plt
from scipy.integrate import odeint

def projectile(V_initial, theta, finlift=True, drag=True):
    g = 9.81
    m = 1.5
    C = .2
    r = .25
    S = np.pi*pow(r, 2)
    rho = 1.204

    time = np.linspace(0, 100, 10000)
    tof = 0.0
    dt = time[1] - time[0]
    fL = rho*g*(4/3*np.pi*pow(r, 3))
    gravity = -g * m
    V_ix = V_initial * np.cos(theta)
    V_iy = V_initial * np.sin(theta)
    v_x = V_ix
    v_y = V_iy
    r_x = 0.0
    r_y = 0.0
    r_xs = list()
```

```

r_ys = list()
r_xs.append(r_x)
r_ys.append(r_y)

for t in time:
    F_x = 0.0
    F_y = 0.0
    if (finlift == True):
        F_y = F_y + fL
    if (drag == True):
        F_y = F_y - 0.5*C*S*rho*pow(v_y, 2)
        F_x = F_x - 0.5*C*S*rho*pow(v_x, 2) * np.sign(v_y)
    F_y = F_y + gravity

    r_x = r_x + v_x * dt + (F_x / (2 * m)) * dt**2
    r_y = r_y + v_y * dt + (F_y / (2 * m)) * dt**2
    v_x = v_x + (F_x / m) * dt
    v_y = v_y + (F_y / m) * dt
    if (r_y >= 0.0):
        r_xs.append(r_x)
        r_ys.append(r_y)
    else:
        tof = t
        r_xs.append(r_x)
        r_ys.append(r_y)
        break

return r_xs, r_ys, tof

```

```
v = 175
```

```
theta = np.pi/4
```

```
def Xdot(x, t):
```

```
    V = x[0]
```

```
    gamma = x[1]
```

```
    H = x[2]
```

```
    R = x[3]
```

```
    g = 9.81
```

```
    rho = 1.225
```

```
    A = 0.45
```

```
    CD0 = 0.3
```

```
    CL = 0
```

```
    e = 0.8
```

```
    taperratio = 1
```

```
    wingarea = 0.45
```

```
    k = 1/(np.pi*taperratio*e)
```

```
    CD = CD0 +k*CL**2
```

```
    L = 0.5*rho*V**2*A*CL
```

```
    D = 0.5*rho*V**2*A*CD
```

```
    m = 1.5
```

```
    V = (((-D-m*g*np.sin(gamma))/m)+V0)
```

```
    gamma = (((L-m*g*np.cos(gamma))/(m*V))+gamma0)
```

```
    H = ((V*np.sin(gamma))+H0)
```

```
    R = ((V*np.cos(gamma))+R0)
```

```

return [V, gamma, H, R]

g = 9.81
CL = 0.8
t0 = 0
tf = 500
V0 = 110
y1 = 453
y2 = 173.5
gamma0 = 1*np.pi/180
H0 = 115
R0 = 110

X0 = [V0, gamma0, H0, R0]
t = np.linspace(0, 1.5)
x = odeint(Xdot, X0, t) #args = (t)

fig = plt.figure(figsize=(8,4), dpi=300)
r_xs, r_ys, tof = projectile(v, theta, True, True)
plt.plot(r_xs, r_ys, 'g:', label="Trajectory for fins actuated upon launch")
r_xs, r_ys, tof = projectile(v, theta, False, True)
plt.plot(r_xs, r_ys, 'b:', label="Trajectory for no fins no wings")
r_xs, r_ys, tof = projectile(v, theta, False, False)
plt.plot(-x[:,3]*t+y1, x[:,2]-y2, 'r--', label="Trajectory for wings actuated")
#plt.plot(r_xs, r_ys, 'k:', label="Gravity")wi
plt.title("Trajectory", fontsize=14)
plt.xlabel("Displacement in x-direction (m)")

```



```
plt.ylabel("Displacement in y-direction (m)")
plt.ylim(bottom=0.0)
plt.legend()
plt.show()
```

Arduino Code – Servo Control

```
#include <Servo.h>

Servo myservo1;
Servo myservo2;

void setup()
{
  myservo1.attach(9);
  myservo2.attach(10);
  myservo1.writeMicroseconds(950);
  myservo2.writeMicroseconds(950);
  delay(8000);
  myservo1.writeMicroseconds(2050);
  myservo2.writeMicroseconds(2050);
  delay(8000);
  myservo1.writeMicroseconds(950);
  myservo2.writeMicroseconds(950);
}
```

References:

- [1] Shevell, Richard S. *Fundamentals of Flight*, 2nd Ed. Englewood Cliffs, NJ: Prentice Hall, 1989.
- [2] Ullman, David. *The Mechanical Design Process*. New York, NY: McGraw-Hill. 5th Edition.
- [3] Sahoo, S., and M.K. Laha. "Defense Science Journal." *Defense Science Journal*, vol. 64, no. 6, Nov. 2014, pp. 502–508.
- [4] D'Amico, William P., Telemetry Systems and Electric Gun Projectiles. Technical Report Army Research Laboratory ARL-MR-499, 2000.
- [5] Massey, K. C., McMichael J., Warnock T., Hay F., Mechanical Actuators for Guidance of a Supersonic Projectile. AIAA 2005-4970. 23rd AIAA Applied Aerodynamics Conference. 6-9 June 2005. Toronto, Ontario, Canada.
- [6] *Vibration Analysis For Electronic Equip.* 1st. ed. 1973, 2nd. ed. 1988, 3rd. ed. 2000 by Dave S. Steinberg, published by John Wiley & Sons Inc.
- [7] VLADAREANU V, BOSCOIANU E-C, SANDRU O-I, BOSCOIANU M. Development of Intelligent Algorithms for UAV Planning and Control. *Proceedings of the Scientific Conference AFASES*. 2016, Vol. 1, p221-226. 6p

[8] Scott, Jeff. *Drag of Cylinders & Cones*. June 5, 2005.

<http://www.aerospaceweb.org/question/aerodynamics/q0231.shtml> (accessed September 10, 2011).

[9] Selig, Michael. "S1223 Test Data." UIUC Wind Tunnel Data (Volume 1). December 5, 1997. <http://www.ae.illinois.edu/m-selig/pd/pub/lsat/vol1/S1223.DRG> (accessed September 10, 2011).

[10] <http://e-feather.blogspot.com/2010/07/gliding-flight-mechanics.html>

[11] <http://www.engineeringarticles.org/milling-machine-definition-process-types/>

Acknowledgements

We would like to thank the Mechanical Engineering Department at the University of the District of Columbia for the use of facilities and support; Dean Shetty for his advising and sharing his expertise on these subjects; Dr. Xu for teaching us design techniques as well as supporting us throughout this process; and Lockheed Martin for sponsoring this project.